TAMPEREEN TEKNILLINEN YLIOPISTO
TAMPERE UNIVERSITY OF TECHNOLOGY

ANZHELIKA KARJALAINEN

# *INTERACTIONS OF JAK2 PSEUDOKINASE AND KINASE DOMAINS IN HEALTH AND DISEASE*

Master of Science thesis

Examiner: prof. Matti Karp
Examiner and topic approved by the Faculty Council of the Faculty of Natural Sciences
on 30th June 2016

# ABSTRACT

**Anzhelika Karjalainen**: Interactions of JAK2 pseudokinase and kinase domains in health and disease
Tampere University of technology
Master of Science Thesis, 46 pages, 2 Appendix pages
May 2017
Master's Degree Programme in Bioengineering
Major: Bioengineering
Examiner: Professor Matti Karp
Keywords: JAK2, kinase, pseudokinase, conformation, interdomain interactions, FRET, labelling, FlAsH-EDT2, V617F, Polycythemia Vera

Homeostasis of the human body depends on the immune system regulated via specific signaling pathways mediated by cytokines. Many cytokines exert their unique effect by the means of JAK/STAT signaling pathway. *Janus Kinase* (JAK) family of enzymes are tyrosine kinase proteins which include 4 members: JAK1, JAK2, JAK3 and TYK2. JAKs consist of four domains: FERM domain and SH2 domain, which are engaged in cytokine-receptor association, and two protein-kinase domains: a pseudokinase domain (JH2) and a canonical tyrosine kinase domain (JH1). Tyrosine kinase domain is responsible for the catalytic activity of the protein whereas the pseudokinase domain was found to have an important role of negatively regulating the tyrosine kinase domain function. JAK kinases are recognized as pharmaceutical targets for treatment of numerous myeloproliferative diseases as well as several types of blood cancer. However, the structure and mechanism of JAK activation and inhibition are still elusive. To design effective pharmaceutical agents, it is of paramount importance to determine the differences in interdomain interactions between pseudokinase and catalytic domains of JAKS in health and disease.

In this study, we apply a novel approach to studying the conformational dynamics between JH2 and JH1. Fluorescence resonance energy transfer (FRET) based on cyan fluorescent protein and new Tetra Cysteine labelling technology that relies on small biarsenical FlAsH-EDT2 dye was used to study the orientational change in JH2-JH1 domains in wild type and under function disruptive mutation, V617F. The FRET measurements were performed in gamma2a cells by acceptor photobleaching. The results demonstrate an altered FRET efficiency in pathogenic constructs which suggests that V617F induces a conformational shift between JH2 and JH1 domains by increasing the distance between the C-terminus of JH1 and the 726-728 residues in the C-lobe of JH2 which brings closer the insertion loop of JH1 domain towards the N-terminus of JH2. Such change might underlie the hyperactivatory effect of V617F mutation and disruption of inhibitory regulation by JH2. Translating our results into precise structural mechanism will help provide better understanding of JAK-specific architectural traits in intramolecular interactions and contribute to design of more effective and selective drugs.

# PREFACE

This thesis is written after the research performed at Faculty of Medicine and Life Sciences, University of Tampere.

I would like to acknowledge the entire crew of Molecular Immunology Laboratory for giving me your hand and a piece of advice when it was most needed. In particular, I would like to thank my supervisor, Bobin George Abraham, and colleague, Henrik Hammaren, for teaching me nearly every knowledge and every skill that I acquired during my work on my Master's thesis research project. Furthermore, I would like to express my sincere gratitude to Olli Silvennoinen for giving me this opportunity, believing in me and sharing your passion and ambition for scientific work.

And above all, I would like to thank my family. I am grateful to my mother and sister who were always there for me to listen to me and cheer me up. And finally, my husband, Timo Karjalainen, who stood by me through the long hours of work at the laboratory and through writing my Master's thesis. I cannot express enough my appreciation for your reassuring support, encouraging confidence and unconditional love.

Tampere, 23.5.2017

Anzhelika Karjalainen

# CONTENTS

1. INTRODUCTION ..... 1
1.1 JAK kinases ..... 3
1.2 Activation of protein tyrosine kinase ..... 6
1.3 JAK kinase inhibitors ..... 7
1.4 Fluorescent proteins ..... 9
1.5 Tetracysteine tag technology ..... 10
1.6 FRET fundamentals ..... 13
1.7 Aim ..... 17
2. METHODS AND MATERIALS ..... 18
2.1 Cloning and constructs generation ..... 18
2.2 Protein expression and purification ..... 20
2.3 Mammalian cell culture, transfection and Western Blotting ..... 21
2.4 Cell labelling ..... 21
2.5 Fixing cells ..... 22
2.6 Microscopy ..... 22
2.6.1 FRET calculations ..... 23
2.7 Statistical analysis ..... 23
3. RESULTS ..... 24
3.1 Construct expression and phosphorylation ..... 24
3.2 Protein purification ..... 24
3.3 FRET ..... 26
3.3.1 Time lapse imaging ..... 26
3.3.2 FRET by acceptor photobleaching ..... 28
4. DISCUSSION ..... 33
5. CONCLUSION ..... 36
REFERENCES ..... 37

APPENDIX A: Cloning sequence

## LIST OF FIGURES

*Figure 1.* *Linear structure of JAK kinase. JAK kinases consist of four main domains: FERM, SH2; JH2 and JH1. The FERM and SH2 domains are subdivided into 5 smaller JAK homology domains. The site of phosphorylation upon JAK activation are marked with yellow stars.....6*

*Figure 2.* *(A) PyMOL ribbon diagram of JH2 (orange) and JH1 (green) domains, based on molecular dynamics simulations by Shan et al. 2014. (B) Differently oriented JH2 domain alone.....6*

*Figure 3.* *A) Color homologs of fluorescent proteins with accentuated central chromophore (CC license). B) Representative 3D image of GFP beta-barrel with fluorophore shown in stick and ball style. The central alpha-helix is shown in purple. The dimensions of GFP are 40 Å long and 30 Å wide (CC license). C) Molecular structure of FlAsH-EDT2 with its dimensions in Ångströms (CC license).....10*

*Figure 4.* *FRET explained. A) Jablonski diagram of FRET (CC license). A fluorescent molecule exists in a ground state before excitation. When energy is applied, a fluorophore is excited to a higher energy level, e.g. $S_1$. An electronic energy level has different vibrational levels. If a fluorophore rises to a higher vibrational level of $S_1$ it quickly undergoes relaxation through internal conversion to the lowest singlet excited state. Energy lost in relaxation process is the reason for wavelength difference between absorption and emission, which becomes red-shifted. Presence of another fluorophore with appropriate absorption spectrum will cause immediate quenching of donor's fluorescence and own excitation from ground state and photon emission. (Abraham 2015); B) FRET efficiency inverse dependency on distance between donor and acceptor. The Föster's critical distance is shown as $R_0$ (Modified from figure adapted with permission of Macmillan Publishers Ltd., © 2008, from (Roy, Hohng, and Ha 2008)) C) Donor and acceptor's fluorescence peaks shown with J ($M^{-1}cm^{-1}$), the spectral overlap of donor's emission wavelength and acceptor's absorption wavelength integrand.....14*

*Figure 5.* *Linear representation of tested constructs. .....20*

*Figure 6.* *Expression and activation of constructs with and without VF .....24*

*Figure 7.* *A) Agarose gel analysis of transposed bacmids helper plasmid and RNA contamination levels. B) PCR verification of Bacmid transposition. The size of construct of interest is 4800 bb, the size of positive controls 1 and 2 is 4100 and 3200 bp, respectively. C) SDS-PAGE gels of purified constructs. The construct molecular*

*weight is 100 kDa, the molecular weight of positive control 1 and 2 is 70 and 35 kDa, respectively. The positions of purified protein bands are marked with black arrows. .....26*

*Figure 8.* *A) and B) Time lapse measurements of CFP fluorescence intensity. The measurements were performed over 15 cycles of 3 minutes by monitoring the intensity of FRET donor. The results are normalized to the first value after subtraction of background signal and presented with standard error. C) and D) Representative images of specificity of labeling with FlAsH-EDT2. The cells exhibited saturation in 514-565 nm channel (FlAsH channel) after 1-1.5h of incubation with FlAsH-EDT2. The unspecific binding was reduced by a washing step with 1,2-ethanedithiol (EDT). The turquoise fluorescent cells in the lowest row of construct 1 and 2 contain a tetracysteine biding motif, whereas the controls do not. The presence of tetracysteine binding motif confers a considerably brighter yellow fluorescence indicative of specific labeling. .....28*

*Figure 9.* *FRET efficiency by acceptor photobleaching in intact cells. A) Construct 1 +/- VF, B) construct 2 +/- VF, C) construct 3 +/- VF. The T- and p-values are obtained with two-sample t-test and presented for constructs with and without VF mutation. The significance of FRET efficiency difference between constructs and controls is more than 99.9%. D), E) and F) representative images of labeling specificity with FlAsH-EDT2. .....29*

*Figure 10.* *FRET efficiency by acceptor photobleaching in fixed cells. A) Construct 1 +/- VF, B) construct 2 +/- VF, C) construct 3 +/- VF. The T- and p-values are obtained with two-sample t-test and presented for constructs with and without VF mutation. The significance of FRET efficiency difference between constructs and controls is more than 99.9%. D) A cartoon representation of JAK2 JH2 (in orange) and JH1 (in green) domains with tetracysteine motives highlighted in red, V617 enclosed in transparent spheres and interactions of fluorophores in every construct are indicated by arrows.....31*

# LIST OF SYMBOLS AND ABBREVIATIONS

| | |
|---|---|
| ATP | Adenosine Triphosphate |
| CC license | Creative Commons license |
| CFP | Cyan Fluorescent Protein |
| CML | Chronic Myelogenous Leukemia |
| EDT | 1,2-ethanedithiol |
| ET | Essential Thrombocythemia |
| FERM | Band-4.1, Ezrin, Radixin, Moesin |
| FlAsH | Fluorescein Arsenical Helix binder |
| FP | Fluorescent Protein |
| FRET | Fluorescence Resonance Energy Transfer |
| GFP | Green Fluorescent Protein |
| IMF | Idiopathic Myelofibrosis |
| JAK | Janus kinase |
| JH1 | JAK Homology 1 (kinase domain) |
| JH2 | JAK Homology 2 (pseudokinase domain) |
| MPN | Myeloproliferative Neoplasm |
| NiNTA | Nickel and Nitrilotriacetic Acids |
| PMF | Primary Myelofibrosis |
| POI | Protein of Interest |
| PTK | Protein Tyrosine Kinase |
| PV | Polycythemia Vera |
| ROI | Region of Interest |
| SH2 | Scr2 Homology domain |
| STAT | Signal Transducer and Activator of Transcription |
| WT | Wild Type |

# 1. INTRODUCTION

Signal transduction is an essential mechanism for cellular survival that allows cells to react to environmental conditions, adopt and communicate. Cellular growth, differentiation, metabolism and proliferation are all the result of cell signaling. Signal transduction is a cascade of biochemical events that involves numerous components. The cascade starts at a receptor protein, usually transmembrane, that is activated by an extracellular signal (ligand) (Kishimoto, Taga, and Akira 1994). Ligand binding induces a conformational change in the receptor protein leading to a signal transduction to a next component of the signaling pathway. Enzymes have a primary role in the signal transduction pathways of modifying other proteins, commonly via phosphorylation, or of being modified. Other molecules can also be involved in the signal transduction, e.g. $Ca^{2+}$, and are termed second messengers, acting as intermediates between enzymes. An important event of signal transduction is modification of gene expression patterns that lead to further activation of protein effectors that finally change cell's morphology or function.

Homeostasis of the human body and its health depend on regulation of the immune system. Immunity and autoimmunity, host defense, inflammation and hematopoiesis regulation occur via specific signaling pathways mediated by cytokines (O'Shea, Gadina, and Kanno 2011). Cytokines are a family of small soluble proteins, peptides or glycopeptides produced by different cell types, including cells of immune system and others, but primarily by helper T-cells and macrophages (Tayal and Kalra 2008; Zhang and An 2007). Cytokines exhibit local and systemic activity by affecting the cells they were secreted by (autocrine), neighboring cells (paracrine) and very distant cells (endocrine) (Zhang and An 2007). Cytokines are classified based on their function, e.g. erythropoietins, thrombopoietins or chemokines; secretion cells, e.g. monokines or lymphokines; and target cells, e.g. interleukins and some interferons (Cytokine sugnaling n.d.). In addition pro-inflammatory and anti-inflammatory cytokines are recognized (Zhang and An 2007). Cytokines possess several distinct properties: pleiotropy (same molecules acting on different cells), redundancy (same function is induced by different molecules) and multifunctionality (same molecule induces different functions) (Tayal and Kalra 2008). As ligands cytokines bind to certain receptor proteins that are divided into six major family groups based on their structural homology: immunoglobulin receptors, interferon receptors (class II), tumor necrosis factor receptors, chemokine receptors, transforming growth factor receptors and hematopoietin receptors (class I) (Wang et al. 2009).

Many cytokines, particularly class I and II receptor cytokines, exert their unique effect by the means of JAK/STAT signaling pathway. Cytokine receptors do not exhibit an intrinsic tyrosine *phosphorylation* activity, i.e. transferring a high energy γ-phosphate

from ATP to a substrate, unlike some tyrosine kinase receptors, for example insulin receptors (Babon et al. 2014). Therefore, other nonreceptor tyrosine kinase proteins are employed (Kishimoto et al. 1994; Rane and Reddy 2000). These tyrosine kinase proteins belong to *Janus Kinase* (JAK) family of enzymes, which includes 4 members: JAK1, JAK2, JAK3 and TYK2 (tyrosine kinase 2) (Babon et al. 2014). JAK kinases are monomers that consist of four main domains: amino-terminal band 4.1, ezrin, radixin, moesin (FERM) domain and a Src homology 2 (SH2) domain, which are engaged in specific receptor subunit association, and tandem kinase domains: a pseudokinase domain (JH2) as well as a tyrosine-kinase domain (JH1). *Janus kinases* received their names from a Roman god with two faces which is analogous to two alike kinase and pseudokinase domains in JAK proteins (Yamaoka et al. 2004). Upon ligand binding a cytokine receptor undergoes oligomerization which leads to juxtapositioning of nearby associated JAKS to form homo- or heterodimers and their activation (Wang et al. 2009). Activated JAK kinases phosphorylate the tyrosine residues on the cytoplasmic region of the receptor. These tyrosine residues comprise a conserved Scr homology site (SH2) which is recognized by signal transducer and activator of transcription (STAT) proteins (Babon et al. 2014; Finbloom and Larner 1995; Rawlings, Rosler, and Harrison 2004). Binding of STATs to the recognition site on the receptor results in their activation by JAK phosphorylation of the conserved tyrosine in the C-terminus of STATS (Rane and Reddy 2000; Rawlings et al. 2004). Activated STATs dimerize and translocate to the nucleus to affect the expression of specific genes by targeting DNA regulatory sequences (Rawlings et al. 2004; Wang et al. 2009).

In the last few decades it has been identified that many malignancies originate from JAK/STAT pathway dysfunction and specific mutations in JAK kinases and STAT transcription factors (Sun and Sun 2014). Mutations leading to disease development are usually characterized as gain-of-function or loss-of-function (O'Shea et al. 2011). Mutations in the JAK bearing alleles result in inactive JAK3 and TYK2. For example, nonsense or frameshift mutations in pseudokinase domain of JAK3 result in truncation of the kinase and are loss-of function leading to X-linked severe combined immunodeficiency (XSCID) (Boggon et al. 2005; Russell et al. 1995). As shown by cancer genome sequencing somatic mutations in JAK1, JAK2 and JAK3 kinases are the primary cause in array of myeloproliferative neoplasms (MPN) and some number of solid tumors (Chen, Staudt, and Green 2012; Lupardus et al. 2014; O'Shea et al. 2011; Sun and Sun 2014). Chronic myelogenous leukemia (CML), polycythemia vera (PV), essential thrombocythemia (ET), idiopathic myelofibrosis (IMF) and primary myelofibrosis (PMF) (Silvennoinen and Hubbard 2015) all belong to the myeloproliferative disorders group represented by elevated proliferation of different hematologic (blood) cell types, increase in proinflammatory cytokines levels, spleen enlargement and incapacitating syndromes (Haleem J. Rasool 2016; Verstovsek et al. 2012). The most characterized valine-to-phenylalanine mutation (shortly V617F or VF) in JAK2 (as well as analogous mutations in JAK1 and TYK2) results in increased phosphorylation of JAK2 substrates

and cytokine-independent signaling. It is found in 95% of PV patients and in 50-60% of ET patients and in some PMF patients (Hammarén et al. 2015; Klampfl et al. 2013). Interestingly, these three different diseases arise from just one mutation. Such phenomenon is attributed to what is now called allele burden of the mutation which is determined as a ratio between mutated and wilt type JAK2 (Passamonti and Rumi 2009). Different 'dosages' of mutant genes are characteristic of certain disease phenotypes. ET phenotype is induced by low dosage of VF mutant JAK2, whereas larger allele burden causes PV phenotype (Scott et al. 2006; Silver et al. 2011). Eventually, increase in allele burden leads to homozygous JAK2 and development of leukemia. That is why *Janus kinases* are attractive pharmaceutical targets and different suppressive drugs were developed in attempt to combat the diseases (Passamonti et al. 2008).

## 1.1 JAK kinases

JAK kinases are relatively large proteins consisting of more than 1100 amino acids and molecular weight of 120-140 kDa (Silvennoinen and Hubbard 2015; Yamaoka et al. 2004). JAK kinases stretch over 7 regions of high sequence homology conserved in mammalian, avian, teleost and insect JAKs. These regions are called JAK homology (JH) domains, numbered 1 to 7 from carboxyl terminus to amino terminus (Figure 1) (Giordanetto and Kroemer 2002; Yamaoka et al. 2004). The 7 JH domains are divided into 4 bigger sites each having their own function. JH1 is a tyrosine kinase domain responsible for the catalytic activity of the protein. JH2 is called a pseudokinase domain because of its structural similarity to canonical kinases but inability to catalyze any reactions. Nearly 10% of kinases encoded by human genome lack essential for catalytic activity consensus sequences and are termed pseudokinases (Min et al. 2015). Nevertheless JH2 domain was found to have an important role of regulating the catalytic domain function by inhibiting its basal activity (Luo et al. 1997; Shan et al. 2014). According to earlier studies (Saharinen and Silvennoinen 2002; Saharinen, Takaluoma, and Silvennoinen 2000) mutations in the JH2 domain lead to abrogated activity of JH1 domain resulting in its hyperactivation and constitutive activity which is the primary cause for MPNs. Therefore, it can be said that pseudokinase domain of JAKs has a tumor-suppressing function (Lupardus et al. 2014). JH3, JH4 and JH5 together comprise the Src homology-2 (SH2) domain whose role is yet unknown but might have a stabilizing role in JAKs conformation (Chrencik et al. 2010) and generally the domain acts as docking site for other tyrosine phosphorylated proteins. The final two N-terminal domains, JH6 and JH7 form a Band-4.1, ezrin, radixin, moesin (FERM) domain (Kohlhuber et al. 1997; Yamaoka et al. 2004). FERM is generally around 300 amino acids long and is involved in receptor interactions. The amino-terminus of JAK proteins is essential for association with common type I and II cytokine receptors, such as hematopoietic growth factor receptors, erythropoietin receptors, interleukins (IL)-2, -3, -4, and -6 and granulocyte-colony-stimulating factor receptors (Giordanetto and Kroemer 2002; Tanner et al. 1995). JAK protein related receptors exhibit two conserved sequences about 8 amino acids long. These sequences carry names 'box1' and 'box2' and

are rich in proline residues. Studies show that mutations in box1 region prevent JAK from stable binding to the receptor and inhibit the downstream signaling (Tanner et al. 1995; VanderKuur et al. 1994).

Despite the successful attempts to purify full length JAK proteins (Duhé, Clark, and Farrar 2002; Ma and Sayeski 2004) the crystalized three-dimensional structure of full length JAKs is unavailable (Giordanetto and Kroemer 2002; Yamaoka et al. 2004). Several groups managed to crystalize separate domains of JAK kinases. For example, in 2014 Lupardus and colleagues crystalized the kinase and pseudokinase domains of TYK2 shedding light on the molecular mechanism by which JH1 is regulated by JH2 and that this regulation is autoinhibitory. A year before that Bandaranayake at al. presented a crystal structure of JAK2 wild type pseudokinase domain and with V617F mutation and characterized their main structural differences. In 2006 a crystal structure of JAK2 kinase domain was obtained by Lucet et al. In 2005 Boggon and colleagues provided a crystal structure of JAK3 kinase domain and described its active conformation that is unique to JAKs family. And Chrencik et al. characterized JAK1 kinase domain in complex with potent pan-kinase inhibitors. However, the listed crystal structures are not of the native sequence or conformation. The wild type as well as apo (ligand unbound) structures could not be obtained, even if the protein could be expressed in baculovirus expression system and had good solubility. The structures presented are usually holo structures in conjunction with some protein kinase inhibitors or containing stabilizing mutations, such as D1023N in TYK2 conferring the kinase inactive (Lupardus et al. 2014), or substitution of hydrophobic residues in solvent-exposed positions (Bandaranayake et al. 2012). Several theoretically generated 3D structures were also produced of the full length JAK2 and separately of its domains that are presented in Figure 2, A and B (Giordanetto and Kroemer 2002; Lucet et al. 2006; Shan et al. 2014).

Structurally the catalytic domain of all typical protein kinases is greatly conserved and comprised of two lobes: N-lobe (residues 840-931 in JAK 2) and C-lobe (932-1132 in JAK 2) that surround the nucleotide binding site (Lucet et al. 2006) (Figure 2, A). The N-lobe includes 5 antiparallel β-strands, numbered β1 to β2, and one α-helix (αC) which is essential for catalytic activity in many kinases (Boggon et al. 2005). The carboxyl-terminal is dominated by 8 α-helices, named αD through αK, 3 shorter helices (3/10 B, C and D) and 6 more antiparallel β-strands (β7 through β11) (Lucet et al. 2006). The connecting part between the two lobes is called a hinge region. Mg-ATP binds JH1 at the nucleotide binding cleft between two lobes which is characterized by a hydrophobic pocket harboring adenine base of Mg-ATP and a polar pocket interacting with ribose and coordinating triphosphates and magnesium (Chrencik et al. 2010). Like in other canonical protein tyrosine kinases (PTKs) the nucleotide-binding site of JH1 contains a threonine and glycine residues that form hydrogen bonds with gamma and beta phosphates of ATP, respectively (Bandaranayake et al. 2012). The ATP interacting glycine is a part of what is called glycine or nucleotide-binding loop with a consensus sequence G-X-G-XX-G, where X stands for any other amino acid. A unique feature

observed only in JAK kinase family is an insertion loop situated between amino acids 1056 and 1078 in JAK2. This loop is presumably involved in regulation of JAK activity through autophosphorylation or in intramolecular interactions with FERM domain (Boggon et al. 2005; Lucet et al. 2006).

JH2 domain starts at 537 phenylalanine and ends at 808 leucine in all JAKs. The structure of JH2 domain of JAK kinases is highly similar to that of the JH1 domain (Figure 2, B) with two lobes and in total 9 α-helices and 8 β-strands (Bandaranayake et al. 2012). However, some essential features required for proper catalytic activity are missing. For example, JH2 domain of JAK2 has a 7 amino acids shorter glycine loop which is non-phosphorylatable and an aspartic acid is missing from the H-R-D motif in the catalytic loop of JH2 which is necessary for phosphorylation (Min et al. 2015). In JH2 the aspartic acid is replaced by asparagine (Bandaranayake et al. 2012). In addition, the catalytic site was found to be abstracted by the activation loop which conformation is characteristic for typical pseudokinases (Toms et al. 2013). Furthermore, a loop between β7 and β8 strands in JH2 is eight amino acids longer than the respective loop in JH1 (Bandaranayake et al. 2012). Nevertheless, unlike other members of JAK family JH2 of JAK2 was found to possess frail catalytic activity. JAK2 JH2 phosphorylates in *cis* Ser523 in SH2-JH2 linker and in *trans* Tyr570 in the β2-β3 loop in JAK2 (Silvennoinen et al. 2013). These residues are present only in JAK2 implying that the activation mechanism for this member of the JAK family is unique. Phosphorylation of these sites is assumed to play role in inhibition of JH1 by JH2 and to stabilize the inactive conformation of JAK2 through electrostatic interactions with basic amino acids on JH1 (Figure 3) (Bandaranayake et al. 2012). The ability for nucleotide binding is preserved in JH2 of all the JAKs and is believed to act as a 'molecular switch' stabilizing the overall conformation of the domain and securing a specific orientation essential for molecular interaction (Babon et al. 2014).

The N-lobe of JH2 domain (exon 12 and 14), β7-β8 loop (exon 16) and the linker between JH2 and SH2 domains harbor most of the function disruptive mutations. Numerous mutations occur in exon 12, which starts at M535 and ends at F547. They include most common substitution of K539L and deletion of E543, others are described in detail in paper by Pietra et al. 2008. V617F mutation is found in exon 14 of JH2 which stretches from S593 to I622 (Ma et al. 2010). The structural differences between wild type and mutated JAKs are quite minor. The V617F mutation in JAK2 is located in the N-lobe of JH2 in the loop between β4 and β5 strands proximal to αC-helix (Dusa et al. 2010). Bandaranayake et al. (2012) identified that the αC helix in JH2-VF is more rigidified due to backbone hydrogen-bonding unlike its somewhat distorted conformation in JH2-WT and is longer by a turn at amino-terminus end. In JH2-VF three phenylalanines, F617, F595 and F594 in the middle of αC-helix in JAK2, form T-shaped pi-stacking interactions. In other tyrosine kinases, e.g. Src and ZAP-70, such stacking was demonstrated to regulate the catalysis by those enzymes (Dusa et al. 2010). Mutation of the phenylalanine at 595 (and F636 in JAK1) position to non-aromatic amino acid disrupts the aromatic stacking interactions and the catalytic func-

tion as well as hyperactivatory effect of V617F mutation decreasing its constitutive activity even by 85%. Mutation of F595 to an aromatic amino acid, however, e.g. tyrosine or tryptophan, reconstitutes the full activity of JAK2 indicating that a bulky hydrophobic residue is essential for maintaining the hydrophobicity of the region and molecular interactions in the αC-helix (Dusa et al. 2010).

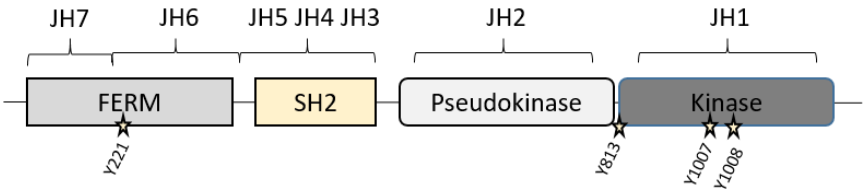


***Figure 1.*** *Linear structure of JAK kinase. JAK kinases consist of four main domains: FERM, SH2; JH2 and JH1. The FERM and SH2 domains are subdivided into 5 smaller JAK homology domains. The site of phosphorylation upon JAK activation are marked with yellow stars.*

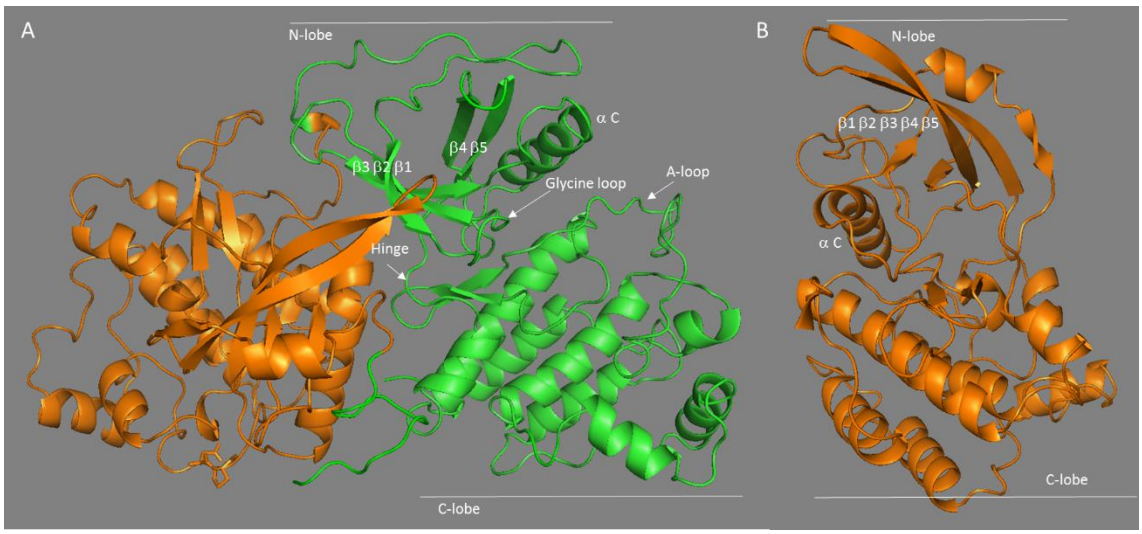


***Figure 2.*** *(A) PyMOL ribbon diagram of JH2 (orange) and JH1 (green) domains, based on molecular dynamics simulations by Shan et al. 2014. (B) Differently oriented JH2 domain alone.*

## 1.2 Activation of protein tyrosine kinase

Activation of JAK tyrosine kinases starts with ligand binding to cytokine receptor inducing a conformational modification in the cytoplasmic region of the receptor leading to formation of multimeric aggregate. The receptor chains accumulation causes juxtapositioning of associated JAK monomers to form homo- or heterodimers (Saharinen and Silvennoinen 2002). Prior to ligand stimulation JH2 domain of JAK kinases is constitutively phosphorylated in residues Ser523 and Tyr570 in JAK2. This substoichiometrical phosphorylation negatively regulates the basal activity of JAK kinase domain by stabilizing the inactive conformation through interaction with positively charged residues on JH1 domain (Shan et al. 2014). Activation of JAK kinase requires phosphoryl transfer

to two tyrosine residues found in the activation loop (Tyr1007 and Tyr1008 in Jak2, 980 and 981 in JAK3) of JH1 domain that play an influential role in regulation of JAK kinase activity. Suppressors of cytokine signaling (SOCS) and protein-tyrosine phosphatases (PTP1B and TCPTP) aim specifically at the activation loop and conserved tyrosine motif to inhibit the cytokine induced signaling (Saharinen and Silvennoinen 2002). The first tyrosine phosphorylation is mediated by lysine and arginine residues in C-helix f JH1 through water-guided hydrogen bonding (Boggon et al. 2005). Phosphorylation of both tyrosines causes the activation loop to be expelled from the catalytic site conferring an active conformation (Babon et al. 2014). Activated JAKs in turn are able to phosphorylate the tyrosine residues on the receptor allowing for further downstream signaling. The precise activation mechanism, however, is still poorly understood. Two models are suggested in favor of in *trans* or in *cis* inhibition by JH2 domain and in *trans* or in *cis* phosphorylation of JH1 domain. The in *cis* autoinhibition mechanism was proposed for the crystalized structure of JH2-JH1 domains of TYK2. It suggests that the N-lobes interactions between pseudokinase and kinase domains rigidify the hinge region between C- and N-lobes in JH1 hindering its elasticity and preventing the orientation of αC-helix and other catalytic elements into a position ready for catalytic reaction (Lupardus et al. 2014). A different mechanism was proposed for JAK2 activation based on SAXS analysis that demonstrated an elongated structure of JH2-JH1 domains indicative of insufficient proximity for in *cis* inhibition (Babon et al. 2014). Another study by Brooks et al. 2014 of growth hormone receptor and its two associated full length JAK2 reveals that upon ligand binding the intercellular part of the receptor undergoes a separation causing the pseudokinase domain to detach from opposing kinase domain and allowing two kinase domains to come in close vicinity for *trans* phosphorylation. Considering that JAK2 possesses two unique sites in JH2 that are constitutively phosphorylated and deemed to be responsible for stabilizing the inhibited state it is presumable that the activation mechanisms are not universal for the JAK kinase family and both models have a right for existence. It is good to point out that two more domains are present in JAKs that might affect the mode of autoinhibition and activation as well as the different receptors that JAKs associate with.

## 1.3 JAK kinase inhibitors

The structure of the catalytic domain in all kinase proteins is highly conserved, that is why it was initially thought that use of kinase targeted therapeutical agents would be accompanied by high toxicity. Furthermore, because the common approach to development of novel drugs was design of competitive ATP inhibitors the prospects of developing selective kinase inhibitors seemed dim. Nevertheless, after long clinical trials there are present 13 FDA-approved kinase inhibitors on the market today (Kontzias et al. 2012). In some cases, the issue with structural similarity was addressed by targeting the kinase superfamily in their inactive conformation that is distinct among them. The fact that the gate-keeper amino acid in the catalytic sites of kinase domains differs among

kinases was exploited to develop specific kinase antagonists (Pesu et al. 2008). However, it turned out that development of strictly specific kinases inhibitors was not required for potent and safe drugs. Numerous kinase antagonists such as dasatinib, sunitinib, sorafenib and others have multiple targets in their mode of action in treatment of cancer and other malignances and such broad applicability provided some unexpected benefits.(Pesu et al. 2008).

The first drug specifically targeted to JAK kinase family which was approved for trials in humans was tofacitinib (CP-690,550) (Ghoreschi et al. 2011). Tofacitinib had significant potency for JAK3, JAK1, some for JAK2 and next to no effect in other kinases (Kontzias et al. 2012; O'Shea et al. 2013). Tofacitinib proved efficacious against allergic diseases and blockade of proinflammatory cytokine production to combat immunological and inflammatory diseases proving especially effective in treatment of rheumatoid arthritis (RA) and can soon be approved for administration to RA patients. However, due to its wide mode of action its side effects included impeded erythropoietin signaling which can result in anemia and neutropenia, as well susceptibility to various infections (Kontzias et al. 2012; Zand et al. 2013). After that several other FDA-approved JAK inhibitors emerged into the market for treatment of rheumatoid arthritis, psoriasis, inflammatory bowel disease and transplant rejection. Ruxolitinib and baracitinib (INCB028050) are JAK1/JAK2 antagonists designed for treatment of myeloproliferative disorders in intermediate and high risk groups but also showed promising results in RA treatment studies (Deininger et al. 2015; O'Shea et al. 2013). Due to similar mechanism of action as of tofacitinib, which blocks many of the cytokines involved in innate immune response, ruxolitinib and baracitinib have similar side effects including anemia and thrombocytopenia (Verstovsek et al. 2012). It was also recently shown that the effect of these drugs, in particular for ruxolitinib, differs with time. In short-term follow-up studies the allele burden of JAK2 V617F mutation was not affected by therapy with ruxolitinib (Silver et al. 2011), whereas another study demonstrated a considerable reduction in allele burden as well as other symptoms, such as splenomegaly, in long-term follow-up studies (Deininger et al. 2015).

Chronic myeloid leukemia (CML) and acute lymphoblastic leukemia (ALL) are targeted with imatinib, sunitinib, nilotinib (AMN107) and dasatinib (BMS-354825). The CML and ALL are cause by constitutively active tyrosine kinase mutant that is translated from an oncogenic fusion gene BCR-ABL. The BCR-ABL gene is a result of fusion between c-ABL and breakpoint cluster gene (BCR) due to translocation of human chromosome 9 and 22 (Tokarski et al. 2006). Imatinib showed high potency against early stage CML, but not advanced, by inhibiting kinase activity of mutant tyrosine kinase. Surprisingly, however, resistance to imatinib treatment is acquired during any stage of the disease due to point mutations at the imatinib binding site in inactive kinase domain of mutant tyrosine kinase (Tokarski et al. 2006). Such resistance was addressed by dasatinib which proved 325-fold more efficacious (O'Hare et al. 2005). Higher effec-

tivity of dasatinib is due to its capability to bind to both inactive and active conformations of the kinase, which demonstrates importance of conformation considerations in drug design (Tokarski et al. 2006).

## 1.4 Fluorescent proteins

In the last few decades the advancement in cell biology research was achieved greatly due to the development of fluorescent proteins (FP). Genetically encoded fluorescent labels enabled the study of biomolecules and biological processes under physiological conditions in their native environment with non-invasive measurement technologies. A great deal of effort was dedicated to engineering of fluorescent proteins with enhanced properties, sensing abilities and increased stability (Abraham 2015). Numerous color variants of fluorescent proteins were engineered to allow visualization of cellular interior in blue to near-infrared range of spectrum (Figure 4, A). Fluorescent switches, optical tweezers, photoactivable FPs, fast-maturing FPs, cell clocks and timers are some of incredibly many tools available for studying cellular organelles and biomolecules' structure and dynamics in spatial temporal manner (Chudakov et al. 2010; Lukyanov et al. 2005).

The first fluorescent protein, green fluorescent protein (GFP), was derived from jellyfish *Aequorea Victoria.* In *A. Victoria* the GFP exists together with photoprotein aequorin in a photogenic organ (Shimomura 1979). Aequorin produces energy required for excitation of GFP via $Ca^{2+}$ triggered biochemical reaction and passes that energy to GFP via Föster-like energy transfer mechanism (Shimomura 1979). GFP molecular weight is 27 kDa with primary structure consisting of 238 amino acids (Abraham 2015). The tertiary structure of GFP is represented by a beta barrel formed by 11 antiparallel β-strands (Chudakov et al. 2010). A distorted α-helix is located along the central axis of the barrel (Figure 4, B). The helix contains three essential amino acids that comprise the main fluorophore: Ser65, Tyr66 and Gly67 (Abraham 2015; Crone et al. 2013). Thanks to beta-barrel structure GFP is a highly stable protein resistant to proteolysis and chemical and thermal denaturation (Abraham2015; Chudakov et al. 2010).

Among naturally occurring fluorescent proteins the amino acids at residues 66 and 67 are conserved, whereas the Ser65 residue varies conferring distinct color homologs. The wild-type variant of GFP was a subject to mutagenesis due to its poor fluorescence at green emission wavelength and brighter fluorescence in UV region of spectrum which is toxic to cells (Heim, Cubitt, and Tsien 1995). Serine to threonine mutation at residue 65 conferred a brighter and more stable green fluorescent protein (excitation/emission – 489/509) which was used as foundation for further development (Abraham 2015). Two mutants were created based on $GFP^{S65T}$: GFPmut1 and enhanced GFP (EGFP; excitation/emission – 488/509) by replacement of phenylalanine at 64 to leucine and codon optimization for expression in bacterial and human cells, respectively (Yang, Moss, and Phillips 1996). Further substitution of tyrosine 66 to histidine resulted in blue fluores-

cent protein (excitation/emission – 382/459) and additional substitution of 145 tyrosine to phenylalanine yielded an enhanced blue fluorescent protein (EBFP; excitation/emission – 380/460) (Heim et al. 1995; Yang et al. 1996). Because the excitation wavelength of BFPs is near UV radiation region, irradiation of cells at that wavelength is toxic. This and other shortages of BFPs hinder its usability in research. Cyan version of GFPs was created by Y66W mutation and then improved to obtain an ECFP (excitation/emission – 434/477; (Heim et al. 1995)). Fluorescent properties of CFP were very inferior in comparison to other engineered FPs, however due to its spectral overlap with YFP, CFP is widely used in fluorescent resonance energy transfer applications (Abraham 2015). Citrine is the most used homolog of EGFP engineered by S65G, V68L, S72A and T203Y mutations. Red variants of FPs, however, could not be derived from GFP protein engineering. That is why the search for red fluorescent proteins among *Anthozoa* species and corals continued until a plethora of red, far-red and orange FPs was discovered (Shcherbakova et al. 2012). mCherry is a modified variant of first RFP mutants which is a monomer with great photostability and is widely used in current cell imaging applications (Abraham 2015).

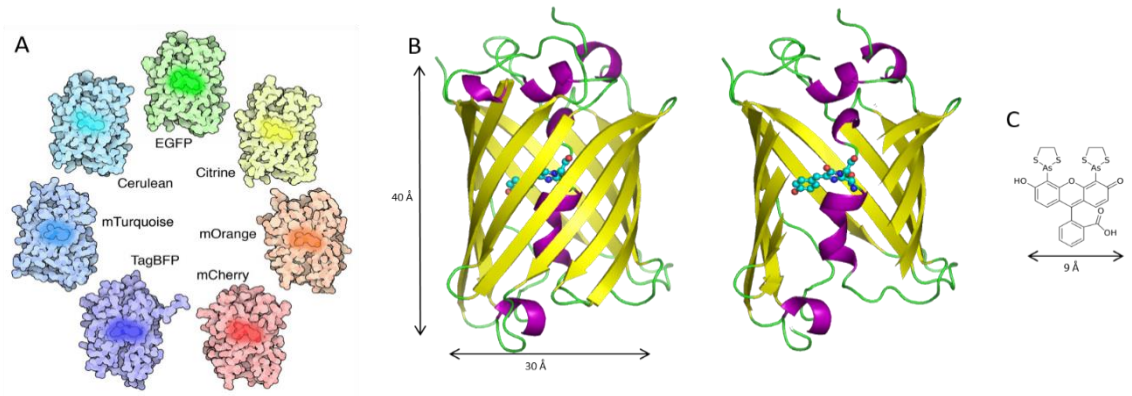


***Figure 3.*** *A) Color homologs of fluorescent proteins with accentuated central chromophore (CC license). B) Representative 3D image of GFP beta-barrel with fluorophore shown in stick and ball style. The central alpha-helix is shown in purple. The dimensions of GFP are 40 Å long and 30 Å wide (CC license). C) Molecular structure of FlAsH-EDT2 with its dimensions in Ångströms (CC license).*

## 1.5 Tetracysteine tag technology

Investigation of proteins of interest (POI) in living cells requires that the native function and structure of POIs are preserved. However, FPs are considerably large biomolecules that, to their disadvantage, can perturb the functional conformation of target proteins. Yet any alterations of fluorescent proteins structure leads to the loss of their fluorescent properties (Wombacher and Cornish 2011).

Attempts were made to reduce the substantial size of FPs by introduction of protein chemical tags. A HaloTag, 30 kDa protein tag, is a slightly altered haloalkane dehalogenase engineered for covalent binding of synthesized ligands (Los et al. 2008). It is responsible for removal of the alkyl group from alkylhalides and its covalent binding to the asparagine residue in enzyme's active site. Mutation of histidine at residue 289 creates a self-modifying HaloTag resistant to hydrolysis of covalent bond with alkyl-fluorophore conjugate (Los et al. 2008). Another development is O6-alkylguanine-DNA-alkyltransferase (hAGT) tags of ~20 kDa size that can be labelled with O6-benzylguanine derivatives conjugated with plethora of fluorescent probes to study membrane as well as intracellular proteins (Gautier et al. 2008; Maurel et al. 2008). hAGT is a DNA repair enzyme engaged in catalysis of cytotoxic alkyl group at $O^6$-locus in guanine to its own cysteine residues (Keppler et al. 2002). Modification of $O^6$-benzyl guanine by attachment of fluorophore results in self-catalyzed labeling of hAGT at its active site. Protein engineering of hAGT allowed to obtain two highly specific tags: SNAP-tag and CLIP-tag that can be fused to POI for substrate-probe conjugate labeling (Johnsson et al. 2011; Keppler et al. 2006). Some of further discoveries include a fusion protein dihydrofolate reductase from *E.coli*, which is 18 kDa protein that can be specifically tagged with trimethoprim derivatives (Hoffmann et al. 2010; Miller et al. 2005); and a acyl carrier protein (approximately 10 kDa) that can be used for selective labeling of surface proteins with synthetic fluorophore compounds (Nathalie George et al. 2004).

All the above listed strategies are still considerably large. More radical steps of reducing the size of genetically encoded reporters lead to development of peptide chemical tags. A peptide chemical tag is a short peptide sequence that can be specifically targeted with a chemical fluorescent compound or be fluorescent on its own. The chemical fluorescent label can interact covalently with the peptide sequence by self-modification or through enzyme intermediate, or non-covalently via high-affinity interactions. Most important properties of small chemical tags should include specificity, minimal molecular weight, high signal to noise ratio, membrane permeability and low cytotoxicity. Peptide tags are advantageous to protein tags due to their small sizes, as little as 2-3 kDa, however specificity of labeling is challenged and can only be improved through enzyme mediated labeling. (Wombacher and Cornish 2011)

Some other approaches in selective chemical labelling were implemented, such as incorporation of unnatural amino acids (Lang and Chin 2014), yet peptide based chemical tags remain the most exploited techniques. To date, the most successful applications of peptide chemical tags were shown with tetracysteine-tag and oligohistidine/nickel complex systems, both reliant on metal-chelation (Soh 2008). Commonly known as His-tag, an oligohistidine sequences consist of 6 to 10 histidine residues. They are characterized by high affinity interactions with nickel and nitrilotriacetic acids (NiNTA) complexes. Apart from broad applications in protein purification technology His-tag system showed

some promising results in selective chemical labelling (Bäumle et al. n.d.; Lata et al. 2006).

The first description of tetracysteine-tag technology was presented by Griffin, Adams, and Tsien in 1998. Their design was based on affinity of arsenoxides (R – As = O) to a couple of adjacent cysteines (Griffin, Adams, and Tsien 1998). In order to increase specificity and reduce cytotoxicity a bis-arsenical fluorescein probe (4',5'-bis(1,3,2-dithioarsolan-2-yl), Fluorescein Arsenical Helix binder (FlAsH), shown in Figure 3, C, was invented with two arsenoxides to target 4 closely-spaced cysteines (Wombacher and Cornish 2011). To further eliminate unspecific binding, labelling with FlAsH can be carried in presence of 1,2-ethanedithiol (EDT). EDT is a disulfide bonds reducing agent that interacts with FlAsH more stably than single cysteine pairs acting as a arsenoxides antidote (Griffin, Adams, and Tsien 1998). Complex of FlAsH and EDT – FlAsH-$EDT_2$, can penetrate the cell membranes and becomes fluorescent upon binding to consensus sequence of tetracoordinate arsenic group CC-XX-CC, where XX is any amino acid. The most optimal and utilized sequence is CC-PG-CC. The binding motif can be inserted at various locations of POI, at either termini or in helical structures (Griffin et al. 1998; Soh 2008).

FlAsH is a yellow fluorescent label with excitation/emission of 508/528 nm. FlAsH consists of two arsenic moieties bound to the xanthene ring of the fluorescein molecule. Derivatives of different colors were designed to enable simultaneous labeling and widen their applications in cell imaging. ReAsH is red colored bis-arsenical dye with excitation/emission of 593/608 nm and CHoXAsH is blue fluorescent molecule with excitation/emission of 380/430 nm (Soh 2008) and others including red BArNile. Improvements of FlAsH fluorescent properties led to development of di- and tetrafluorinated FlAsH (F2FlAsH and F4FlAsH). These two derivatives are superior to FlAsH in many physical aspects, such as better absorbance, higher quantum yield, better photostability, in fact 50 times higher, and others. Additionally, F4FlAsH excites at 528 nm and emits light at 544 nm, which is an intermediate region in visible light spectrum between FlAsH and ReAsH creating a new color variant (Soh 2008; Spagnuolo, Vermeij, and Jares-Erijman 2006). F2FlAsH and F4FlAsH as well as FlAsH and ReAsH can be utilized as donor-acceptor pairs for fluorescence resonance energy transfer (FRET) experiments (Soh 2008). Another improved analog of ReAsH that can act as a FRET partner for FlAsH is AsCys3. The advantage of using AsCys3 is a longer interatomic distance between two arsenic atoms, particularly 14 Å in comparison to 6 Å between ReAsH arsenic moieties. It is thought to allow more selectivity when multiple reporters are used to label several POI (Haishi Cao et al. 2007). AsCys3 binds CCKAEAACC with high affinity (Kd = 80 ± 10 nm) with red-shifter emission values of 568-576 nm (Haishi Cao et al. 2007; Soh 2008). The consideration of rigid structure between two arsenical species in FlAsH dyes and consequent limitation in fluorophore choice led to a new engineering design where the xanthene ring acts as anchoring point between arsenic atoms

and a fluorophore. Such structure, collectively called as SplAsH, enables generation of multiple color homologs, such as SplAsH-Alexa594 and many others (Bhunia and Miller 2007).

Advancement in engineering of bis-arsenical labels and chemical tags created a remarkable toolbox for bioanalytical research. It was possible to achieve specific visualization of two RNA polymerase subunits from whole cell lysate (Chen et al. 2007). Tour et al. (2007) were able to precisely monitor calcium ion fluxes through gap junction by generating a $Ca^{2+}$ indicator with impressive affinity and kinetics. Despite some drawbacks of first FlAsH dyes, modern FlAsH derivatives possess some outstanding properties and can make significant contribution to progress in cell biology research.

## 1.6 FRET fundamentals

Fluorescence resonance energy transfer, also known as Föster resonance energy transfer, is a powerful technique that enabled numerous discoveries in biology, chemistry and other disciplines. In fact, the optimal FlAsH binding motif was identified by the means of FRET between GFP and ReAsH bound to randomized sequences containing four cysteine residues (Soh 2008). FRET is a phenomenon that arises from intrinsic property of a fluorophore in excited state to transfer its energy to another fluorophore instead of emitting a photon (Figure 4, A). Provided that a sufficient overlap of emission/excitation spectrum, J (λ) exists between two fluorophores the energy accepting fluorophore will become fluorescent (Figure 4, C; (Hussain n.d.; Sekar and Periasamy 2003; Abraham 2015).

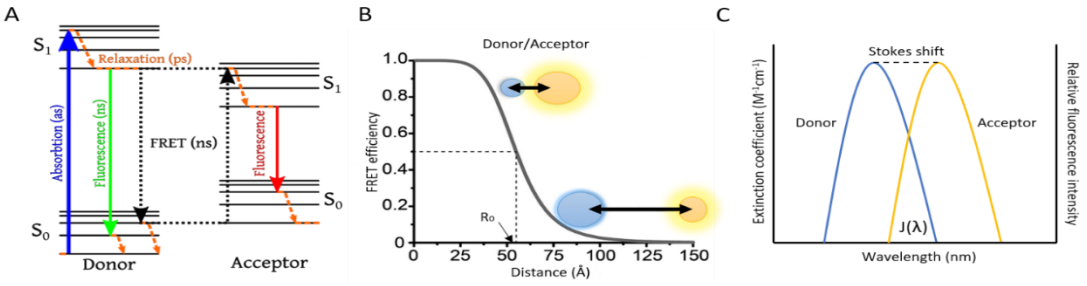


***Figure 4.*** *FRET explained. A) Jablonski diagram of FRET (CC license). A fluorescent molecule exists in a ground state before excitation. When energy is applied, a fluorophore is excited to a higher energy level, e.g. $S_1$. An electronic energy level has different vibrational levels. If a fluorophore rises to a higher vibrational level of $S_1$ it quickly undergoes relaxation through internal conversion to the lowest singlet excited state. Energy lost in relaxation process is the reason for wavelength difference between absorption and emission, which becomes red-shifted. Presence of another fluorophore with appropriate absorption spectrum will cause immediate quenching of donor's fluorescence and own excitation from ground state and photon emission. (Abraham 2015); B) FRET efficiency inverse dependency on distance between donor and acceptor. The Föster's critical distance is shown as $R_0$ (Modified from figure adapted with permission of Macmillan Publishers Ltd., © 2008, from (Roy, Hohng, and Ha 2008)) C) Donor and acceptor's fluorescence peaks shown with J ($M^{-1}cm^{-1}$), the spectral overlap of donor's emission wavelength and acceptor's absorption wavelength integrand*

The process of energy transfer occurs nonradiatively due to long distance dipole-dipole coupling between two molecules. FRET phenomenon is distance dependent and takes place more efficiently within 10 nm radius (10-100 Å). The distance at which the FRET efficiency is 50% is called Föster's critical distance, indicated as $R_0$, and is dependent on spectroscopic properties of donor-acceptor pair (Figure 4, B; (Sekar and Periasamy 2003)). FRET is also dependent on the transitional orientation of two fluorophores relative to each other. Therefore, the efficiency of the energy transfer is calculated based on the distance separating two fluorochromes which is raised to the inverse sixth power due to the orientation of the donor emission dipole moment with acceptor's excitation dipole moment (Periasamy, Day, and American Physiological Society 2005).

$$E = \frac{(R_0)^6}{(R_o)^6 + (R)^6}, \quad (1)$$

Formula 1 relates the separation distance between two fluorophores to the energy transfer efficiency (Gu et al. 2004; Visser, Vysotski, and Lee 2011), where $R_0$ is the Förster's critical distance. $R_0$ can in turn be evaluated by the following formula:

$$R_0 = \sqrt[6]{0.2108[k^2 Q_D n^{-4} J]}, \quad (2)$$

where $Q_D$ is the quantum yield of the donor fluorescence without acceptor. The quantum yield of mTurquoise Cyan fluorescent protein is 0.84 (Goedhart et al. 2010). As a remark, the quantum yield for 250 nM FlAsH bound to tetracysteine motif in phosphate-buffered saline at pH 7.4 is 0.49. $k^2$ is dipole orientation factor. It depends on the angle between fluorophores, but is often assumed to be 2/3. n is refractive index of intervening medium, which could be approximated to the refractive index of water equal to 1.330. By using a salt solution dissolved in water the refractive index can be rounded to 1.4 (Visser et al. 2011). Finally, J ($M^{-1}cm^{-1}nm^4$) is the spectral overlap of donor's emission wavelength and acceptor's absorption wavelength integrand. J depends on the molar extinction coefficient which for FlasH-EDT2 was determined in the range from 30000 to 80000 $M^{-1}cm^{-1}$ (Griffin et al. 1998). The molar extinction coefficient of YFP is 62000 $M^{-1}cm^{-1}$ (Adams et al. 2002). J also is dependent of the cumulative of donor's emission spectrum normalized to the area of 1 and can be calculated using formula 3.

$$J(\lambda) = \int F_D(\lambda)\varepsilon_A(\lambda)\ \lambda^4 d\lambda, \tag{3}$$

where $F_D(\lambda)$ is wavelength function of donor emission, $\varepsilon_A(\lambda)$ is wavelength function of acceptor excitation (Abraham 2015).

A common method used to identify the distance separating two fluorophores based on the measured FRET efficiency is lifetime measurements or time resolved fluorescence measurements (Abraham 2015). A lifetime of fluorescent molecule represents the time it remains in the excited state before returning to the ground state. If no energy transfer occurs the fluorophore returns to it ground state slower (formula 4). If, however, another fluorophore is present the donor fluorophore drops to the ground state faster. The relationship between FRET represented as a rate of energy transfer and lifetime of a fluorescent molecule can be seen in formula 5.

$$\tau_D = \frac{1}{(k_r + k_{nr})}, \tag{4}$$

$$\tau_{DA} = \frac{1}{(k_r + k_{nr} + k_t)}, \tag{5}$$

where $k_r$ is the rate of radiative decay, $k_{nr}$ is the rate of nonradiative decay and $k_t$ is the rate of energy transfer. Based on the difference between the lifetime of a fluorophore with and without the influence of energy transfer the real FRET efficiency can be calculated as follows:

$$E = 1 - \frac{\tau_{DA}}{\tau_D}, \tag{5}$$

The most utilized approach to FRET measurements, though, is steady state measurements. The reason for higher preference among investigators is the possibility to use a

conventional confocal or fluorescence microscope as well as steady-state spectrofluorometer (Abraham 2015). This way of FRET determination received its name due to the fact that when a sample is excited a steady-state among the fluorophores in the excited and ground energy levels is achieved in nanosecond time. The intensity, therefore, of the fluorescence is detected in steady state (Periasamy et al. 2005). The fluorescence measurements can be carried out as measurements of sensitized emission by either two-channel or spectral imaging or as measurements by acceptor photobleaching. The basis for sensitized emission analysis lies in direct registration of the donor and/or acceptor fluorescence in presence of each other after excitation of donor. Occurrence of FRET is evaluated by the decrease in donor fluorescence in presence of acceptor (Berney and Danuser 2003). Acceptor photobleaching relies on the fact that the fluorescence intensity of donor fluorophore is quenched in the presence of acceptor. If the acceptor fluorophore is subjected to photobleaching the donor fluorescence is recovered (Abraham 2015).

To gain valuable quantitative information from FRET measurements it is essential to generate appropriate controls and evaluate the bias caused by bleed-through in excitation and cross-talk in emission. Such biases arise from signal interference between acceptor excitation with donor excitation and donor emission with acceptor emission and are often difficult to separate (Berney and Danuser 2003). Qualitative measurements with a purpose of assessment of apparent protein-protein interactions, however, can be obtained without excessive controls and are a means by which the aim of this study is achieved.

## 1.7 Aim

Treatment of diseases caused by mutations of JAK kinases for years has been accomplished by the means of type I JAK inhibitors. Type I JAK inhibitors bind catalytic ATP-binding site in the active conformation of the kinase. Despite some positive results in disease treatment the activity of type I inhibitors increases autophosphorylation leading to some adverse downstream signaling. In expectation of more effective results type II inhibitors were developed targeting the JAK kinase domain in an inactive conformation. Yet, neither of the aforementioned pharmaceutical agent groups were able to completely prevent the detrimental effects of JAK kinase mutations. In order to design effective pharmaceutical drugs, which can differentiate between active and inactive states of JAK kinases as well as mutant vs wild-type, it is of paramount importance to determine the three-dimensional structure of JAKS as well as activatory/inhibitory mechanisms of pseudokinase and kinase domains.

The aim of this study is to conduct a qualitative analysis of JAK2 pseudokinase and kinase domains interactions in health and disease. By creating JAK2 JH2-JH1 DNA constructs fused with fluorescent tags we perform Fluorescence Resonance Energy Transfer (FRET) measurements *in vitro* and in live cells by acceptor photobleaching and time lapse imaging. To preserve the functional and structural integrity of the target protein we used a tetracysteine tag technology, which is the smallest genetically encoded tag capable of site-specific labelling inside living cells. FlAsH-EDT2 and cyan fluorescent protein are used as a FRET pair. The labelling procedure is methodically optimized for our specific constructs and cells. This approach has never been implemented in the study of JAK kinases. Such knowledge could bring us closer to visualizing the structural changes in pathogenic and wild type JAK2 kinase and possibly contribute to development of novel drugs specific for mutant JAKs.

# 2. METHODS AND MATERIALS

## 2.1 Cloning and constructs generation

Ten DNA constructs with and without V617F mutation were created. The DNA sequence of JH2-JH1 was fused with cyan fluorescent protein (CFP) and inserting tetracysteine motif at three different loci. The JH2-JH1 sequence starts at 535 methionine followed by 536 valine and ending with 1132 glycine followed by a stop codon. The JH2-JH1 sequence is presented in Table 1, Appendix A. Construct 1 +/- VF, construct 2 +/- VF, construct 3 +/- VF and corresponding controls are shown in Figure 4. In constructs 1 and 3 the CFP is fused without a linker to the amino-terminus of JH1, in construct 2 CFP is fused to the carboxyl terminus of JH2. An optimized tetracysteine sequence was identified for efficient labelling with FlasH-EDT2 where four cysteines are separates by a proline and glycine motif – CCPGCC (Adams et al. 2002). In construct 1 the tetracysteine motif was added right before 536V without a linker preceded by a start codon. In construct 3 CCPGCC sequence was inserted in JH2 domain at position between N726 and K728. The asparagine and lysine were replaced with two terminal cysteines of CCPGCC sequence and the proline between N and K is completely removed so that the protein is only 3 amino acids longer as such: K726C-CPGC-N728C. In construct 2 the tetracysteine motif is inserted in a similar manner so that the 1053 lysine and 1055 are replaced with cysteines and 1054 serine is removed and CPGC is inserted: K1053C-CPGC-K1055C. The DNA sequence for tetracysteine binding site was tgt tgc ccg ggc tgc tgt harboring a Sma1 restriction site in ccg ggc for verification of insertion. The controls are JH2-JH1-CFP constructs without CCPGCC motif. All constructs contained a thrombin cleavage site followed by a 6 x His tag for protein purification with Nickel beads.

The constructs were generated by the means of overlap extension PCR (soePCR) for introduction of CFP and QuickChange site-directed mutagenesis (Stratagenes) for introduction of tetracysteine sites and VF mutation. In soePCR sequences are amplified so that an overlap region is created. The sequences are then joined by complementarity in the first 10 cycles after which primers are added and the whole sequence is amplified. In site-directed mutagenesis the primers contain a target mutation and complements to the original sequence on both sides of the mutation. The whole plasmid is amplified with forward and reverse primers after which the original sequence is digested by Dpn1 restriction enzyme which is able to distinguish the new sequence due to a nick caused by PCR. Construct 1: human wild type JAK2 was amplified from 536 to 1132 residues with forward primer - tatagtcgacatgtgttgccctggctgctgtatggtgtttcacaaaatcag (1) including

start codon, tetracysteine sequence and Sal1 restriction site and reverse primer - ctcgcccttgctcaccattccagccatgttatcccttatttg creating an overhang with CFP. CFP sequence was amplified with forward primer - ggatcaaataagggataacatggctggaatggtgagcaagggcgag creating an overhang with JH1 and reverse primer - tatagcggccgctcag-tggtgatggtgatgatggctgccgcgcggcaccagcttgtacagctcgtccatgccgag (2) including thrombin, His tag and Not1 restriction site. The sequences are joined in soePCR and amplified with (1) and (2). Construct 3: human wild type JAK2 was amplified from 536 to 1132 with forward primer - tatagtcgacatggtgtttcacaaaatcagaaatgaa containing a start codon and Sal1 site and a reverse primer - ctcgcccttgctcaccattccagccatgttatcccttatttg creating an overhang with CFP. The same CFP amplicon was used for construct 3. The tetracys-teine motif was inserted with forward primer - gaatgcattgaatgttgcccgggctgctg-taatttaaatttggcaacagacaaatg and reverse primer - gccaaatttaaattacagcagcccggg-caacattcaatgcattcaggtggtacccatgg. Construct 2: JH2-JH1 sequence was generated by amplification with forward primer - ctcggcatggacgagctgtacaa-gatggtgtttcacaaaatcagaaatgthat creates an overhang with carboxyl-terminus of CFP and reverse primer - tatagcggccgctcatccagccatgttatcccttatttgatcc (3) that inserts Not1 re-striction site. CFP was amplified with forward primer - tatagtcgacatgcatcatcaccatcac-cacctggtgccgcgcggcagcgtgagcaagggcgaggag (4) introducing a Sal1 restriction site, 6xHis tag and a thrombin cleavage site, and a reverse primer catttctgattttgtgaaacac-catcttgtacagctcgtccatgccgag creating a JH2 overlap region. The CFP and JH2-JH1 am-plicons were extended in soePCR with (3) and (4). The tetracysteine motif was inserted with forward primer - cacatacattgagtgttgcccgggctgctgtagtccaccagcggaatttatgcgtatg and reverse primer - cgctggtggactacagcagcccgggcaacactcaatgtatgtgaaaagttcatacag. The VF mutation was introduced with the following primers: atggagtatgtttctgtggagacgagaa-tattctgg and tcgtctccacagaaacatactccataatttaaaacc.

The constructs were cloned into pFastBac1 (Invitrogen) plasmid for insect cell culture and into pEGFP (Addgene) plasmid for mammalian cell culture. The constructs were restricted at Sal1 at 5’ and Not1 at 3’ restriction sites with Sal1 and Not1 fast digest enzymes (Thermo Fisher Scientific, FD0644, FDo593) and ligated with T4 DNA ligase (BioLabs, M0202S). PCR and restriction reactions were followed by gel electrophoresis for DNA purification and enzyme removal. The ligation product was heat inactivated for 10 minutes at 60 ºC and then directly transformed into XL1Blue cells. Five to ten colonies were picked for miniprep DNA extraction. Cloning was verified by restriction reaction and sequencing with Big Dye Terminator v1.1 Cycle Sequencing kit (Applied Biosystems, Foster City, CA). Midipres of the verified constructs were created and di-luted to the final concentration of 200 ng/µL.

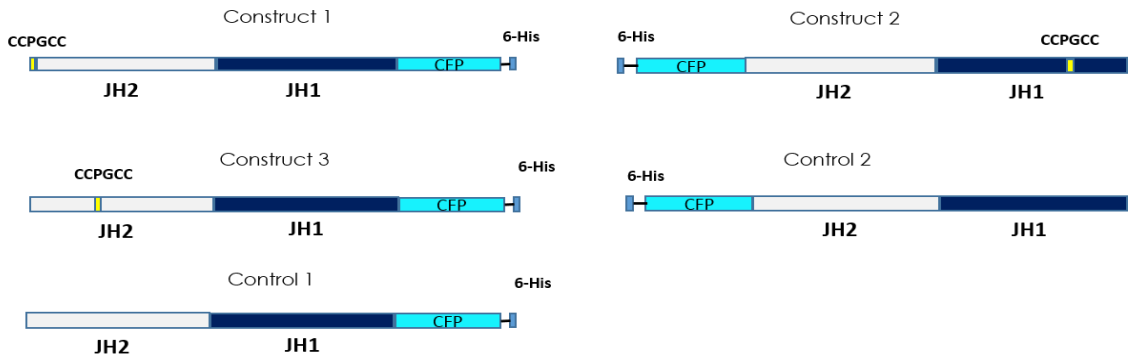


***Figure 5.*** *Linear representation of tested constructs.*

## 2.2 Protein expression and purification

The constructs and their controls were expressed with Bac-to-Bac expression system in baculovirus-infected *Spodoptera frugiperda*-9 (SF9) cells. The pFastBac plasmids with constructs of interest were transformed into DH10Bac *E.coli* strain where a recombinant baculovirus shuttle vector (bacmid) bMON14272 (138 kb) was generated by transposition of mini-Tn7 site in pFastBac with mini-*att*Tn7 site in bacmid. Transformed colonies were kanamycin, tetracycline and gentamycin resistant and could be identified by appropriate color. Intact bacmid vector contains a LacZα gene that allows digestion of chromogenic substrate, X-gal, under IPTG inducer conferring a blue color. A vector with recombined sequence of interest, on the other hand, is white. Verification of sequence transposition in extracted Bacmid DNA was performed by PCR with M13 forward and reverse primes and visualized on 7% agarose gel. PCR product of untransposed Bacmid appears on 300 bp band, PCR product of pFastBac1 without an insert appears at 2300 bp band or higher depending on the size of target insert. Bacmid helper plasmid and RNA contamination levels were visualized with 5% gel electrophoresis. The helper plasmid appears at approximately 10 kb. RNA contamination shows on the bottom of DNA ladder, construct repeats with the least RNA contamination were chosen.

The recombinant bacmid vector was isolated and transfected into insect cells. SF9 cells were cultured in HyClone SFX-insect media at 27ºC in a shaking incubator and subcultured every 72 hours at precisely same time. The cells were transfected with 1-2 microliters of bacmid DNA with Cellfectin reagent (Thermo Fisher Scientific, 10362100) in 6-well plates. The virus expansion was carried out every 3 days from P1 to P2 by centrifugation (4 000g, 1 min, +4ºC) of infected cells and collection of virus containing supernatant. The concrete manual can be obtained from Invitrogen (cat. number 10359-016) Bac-to-Bac Baculovirus expression system. SF9 cells infection was done at 1% virus concentration. Virus stocks were stored t +4ºC up to six months. Test production of target proteins was carried out at 5% or 10% P3 virus concertation in 50 mL SF9 cell cultures at 4-5 x $10^6$ cells/mL density.

Protein purification was conducted by the means of His-tag NiNTA resin beads. Test production cell cultures were collected by centrifugation (4 000g, 3 min, +4ºC) and re-suspension in His lysis buffer (20 mM Tris pH 8 or 8.5, 500 mM NaCl, 20% glycerol, 30 mM imidazole) with the following protease inhibitors: Sodium Vanadate (10 µL/mL), Aprotinin (6 µL/mL) and PMSF (10 µL/mL). For proper lysis cells were rotated for 45 minutes at +4ºC and sonicated 3 times for 30 seconds in 5-seconds pulses at 29% amplitude. Lysed cells were centrifuged at 10 000g for 1 hour. The NiNTA beads were washed 3 times with lysis buffer without inhibitors. The supernatant containing protein mixture was added to the washed beads and rotated for 2 hours at +4ºC. The beads were then washed 3 times to remove the unbound proteins and the protein of interest was eluted 3 times with elution buffer (lysis buffer with 0.25 M imidazole). The purified proteins were verified by running on 10% SDS-PAGE gels with 4 x SDS sample buffer and dyed with instant blue for ≥ 30 minutes.

## 2.3 Mammalian cell culture, transfection and Western Blotting

Human fibrosacroma gamma2a cells were chosen for in cell experiments due to endogenous JAK2 deficiency. The cells were cultured in Dulbeco's Modified Eagle Medium with 10% FBS, 0.5% PenStrep and 1% Glutamate and subcultured every 3-4 days. Twenty-four hours before transfection cells were seeded in 6 well plates at 1-2 $x10^5$ cells/well (24-well plate 5 $x10^4$ cells/well). Cells were transfected with Fugene HD (Roche) according to manufacturer's instructions with 600 and 1200 ng of DNA per well (75-150 ng in 24-well plate). After 24-48 hours, the cells were lysed with lysis buffer (50 mM TRIS-HCl, pH 8, 150 mM NaCl, 100 mM NaF, 10% (v/v) glycerol, 1% (v/v) Triton-X) containing protease inhibitors (Sodium Vanadate, Aprotinin, Pepstatin and PMSF). The expression of the constructs of interest and protein phosphorylation was analyzed with Western blotting with anti-pJAK2 1007 and 1008 (Cell Signaling Technology) and anti-His antibodies (Invitrogen).

## 2.4 Cell labelling

Fluorescence resonance energy transfer was performed in live and fixed gamma2a cells. For live cell experiments, the cells were seeded in glass-bottomed cell dishes with cover slips (35mm) in phenol red free medium to achieve 40-50% confluency at the moment of transfection (1-2$x10^5$cell/well). For fixed cell experiments, the cells were seeded at the same density in 6-well plates containing coverslips. Transfection was followed by 48 hours incubation period. Cells were washed 2 times with 1-2 mL of prewarmed labelling buffer - 1x Hank's Balanced salt solution (HBSS, Thermo Fisher Scientific, 14025092). FlasH-EDT2 (664.5 g/mol) probe (Santa Cruz Biotechnology, 212118-77-9) was diluted in dimethyl sulfoxide (DMSO) to 1 mM concentration and the stocks were stored in 10 µL aliquots at -20ºC protected from light. 25 mM of 1,2-ethanedithiol (EDT) was diluted in DMSO right before labeling. Per sample: 1 µL of 25 mM EDT

and 1 µL of 1 mM FlasH were incubated protected from light for 5-10 minutes. FlasH/EDT was mixed with 100 µL HBSS and incubated for 5 minutes. The remaining 900 µL of HBSS was added to the mixture to obtain final FlasH concentration of 500 nM. HBSS was aspired from cells, FlasH-EDT2 HBSS mixture was added and incubated for 1-1.5 hours at 37ºC protected from light. To remove unbound label the labeling solution was replaced with 250 µM EDT and the cells were incubated for 10-15 min at 37ºC protected from light. After incubation, the cells were washed 2-3 times with prewarmed HBSS. If the cells were imaged immediately they were left in HBSS, else cells were kept in phenol red free complete medium for up to 48 hours.

## 2.5 Fixing cells

Labeled cells were fixed using 4% paraformaldehyde. The coverslips were washed 2 time with room temperature phosphate buffered saline (PBS) and incubated with freshly prepared 4% paraformaldehyde for 10 minutes at room temperature. Cells were washed again with PBS and mounted on glass slides. The slides were washed with 100% ethanol. One drop of mounting medium was applied to the center of the slide and the coverslips were placed cells down onto the glass slides. The mounted slides were cured for 24 hours at room temperature in a dry and dark area and store at 4ºC for up to a month.

## 2.6 Microscopy

Fluorescence time series imaging and FRET by acceptor photobleaching were performed with Zeiss LSM 780 confocal microscope. The microscope was equipped with an incubator for maintenance of physiological conditions during the procedures. 62X water based immersion objective with 1.2NA was used for live cell imaging and 62X oil based immersion objective with 1.4NA was used for fixed cell imaging. The microscopy setup was kept constant in every experiment. Acquisition was performed at 12 Bit image. Gain (sensitivity of photomultiplier) was set at 500 – 800, pinhole was kept at 90 µm based on the best noise to fluorescence ratio, digital offset at zero, digital gain at 1.1, laser power was kept low at 1-2% to minimize photo bleaching of the samples during imaging.

Time lapse fluorescent imaging was carried out over a 20-30 cycles (1 – 1.5-hour period) with 3-minute increments between imaging. FlAsH-EDT2 was added after the first cycle. Measurements were done in four channels: CFP (405-455 nm), FRET (405-520 nm), FlAsH (514-565 nm) and bright field. FRET by acceptor photobleaching was performed with time series of 15 cycles with 0 milliseconds intervals between imaging with number of iterations equal 50. Bleaching was started after the first 5 cycles. Zoom factor was kept equal at 3. Frame size small (512XY), high resolution at optimal, averaging at 1 and scanning speed at maximum to overrun the diffusion of the POI. Bleaching was done to full cells and a specific region of interest for intensity data extraction

was selected at image processing stage. The image processing was done with ImageJ software.

### 2.6.1 FRET calculations

Upon addition of FlaH-EDT2 the CFP fluorescence intensity in the expressed constructs in quenched provided that the probe is specifically bound at tetracysteine motif. When FlasH-EDT2 is bleached the donor fluorescence recovers to an extent dependent of the distance between two fluorophores. The FRET efficiency is calculated with the following formula.

$$E = \frac{I_{after} - I_{before}}{I_{after}} \times 100, \quad (1)$$

where E is apparent FRET efficiency in %, $I_{after}$ is the mean donor intensity of following 5 measurements after bleaching and $I_{before}$ is the mean donor intensity of 5 measurements before bleaching.

## 2.7 Statistical analysis

Statistical analysis was performed with SPSS software. The statistical significance (p-value) of changes in mean FRET intensity between constructs of interest relative to control and between wild-type and VF mutants was calculated with Student t-test. The normality of data was assessed with Shapiro-Wilk test and analysis of z-values of skewness and kurtosis.

# 3. RESULTS

## 3.1 Construct expression and phosphorylation

Expression and activation of +/- VF constructs was analyzed by Western Blotting against anti-pJAK2 Y1007 and Y1008 antibodies and His-tag antibodies. The constructs were transfected at two concentrations: a – 75 ng/well, b – 150 ng/well. A negative control of untransfected cells was used to identify background noise. The constructs are expressed in mammalian cells and appropriate size was observed in western blot. However, the expression levels vary and the N-terminus CFP fusion proteins appear to be expressed more. This difference can be addressed by improving the quality of the plasmid and by titration of DNA concentrations to identify the suitable concentration for transfection. It is evident from Figure 6 that phosphorylation of JH1 Y1007 and Y1008 is not consistent among the constructs either, but is the same between wild type and corresponding pathogenic versions. Construct 2 and control 2 appear to be activated to a small degree in both wild type and VF mutants. It should be noted that the expression of constructs with C-terminus CFP is lower in both +/- VF, and due to this, a higher concentration of DNA was used for FRET experiments.

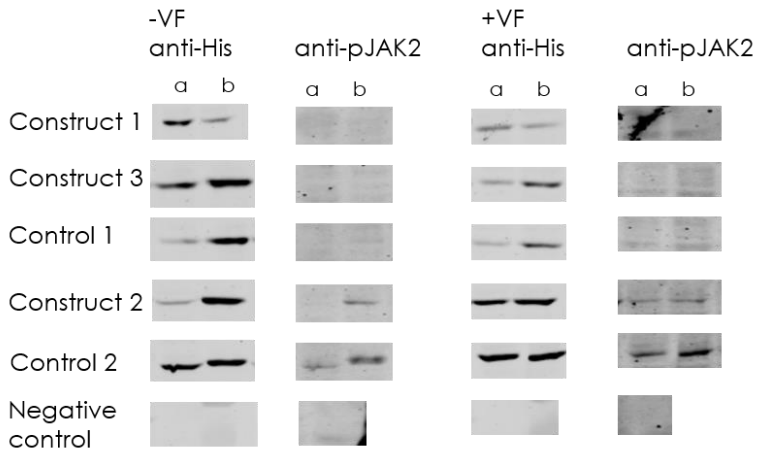


***Figure 6.*** *Expression and activation of constructs with and without VF*

## 3.2 Protein purification

Protein purification of five constructs of interest without V617F mutation was carried out along with 2 positive controls which could previously be successfully purified. Positive controls used in the experiment were two wild type JH2-JH1 domains of JAK2

(positive control 1) and one wild type JH1 domain of JAK3 (positive control 2). Preceding baculovirus production, generated bacmids were analyzed for gene of interest sequence insertion with 5% agarose gel analysis and PCR. While it is almost impossible to visualize the entire bacmid vector with gel electrophoresis due to its very large size (136 kb) the baculovirus expression system includes another plasmid, a helper plasmid, bearing a transposase enzyme which facilitates *in trans* transposition (Barry 1988). The helper plasmid is over 10 kb in size but is still visible when run on low density 5% agarose gel as shown in Figure 7, A. High molecular weight bacmid plasmid is too large to depart from the wells on agarose gel but can still be distinguished right underneath them. The insertion of sequence of interest was verified by PCR with M13 primers. The expected size of PCR product of constructs 1, 2 and 3 (marked as 1, 2, 3 in the Figure 7, B) and controls 1 and 2 (denoted as ctrl 1 and ctrl 2) was 4800 bp, 4100 bp of positive control 1 and 3200 bp of positive control 2. The DNA bands of the correct size appear above a bright 3000 bp ladder band in Figure 7, B.

The expected protein molecular weight of the constructs was 100 kDa which can be found on the SDS page ruler ladder right above the black 70 kDa mark. The size of positive control 1 was 70 kDa and positive control 2 was 35 kDa. Samples for SDS-PAGE gel were taken after every step of protein purification for monitoring errors during the procedure. The first lane on the gels corresponds to whole cell lysate after sonication. Second lane represents the sample of cell pellet after centrifugation of cell lysate. The third lane represents the unbound protein after incubation with NiNTA beads and centrifugation. The forth lane shows presence of any protein after the first washing step. The lanes from 5 to 8 are the 3 elution steps and the last lane are the beads suspended in elution buffer.

As it can be seen from the images (Figure 7, C), purification of the target constructs was unsuccessful. The arrows indicate where the protein band would be expected to be. By comparing to the positive controls, we can notice a considerable amount of protein already in the whole cell lysate and pellet samples. As there's almost no protein visible in lanes 3 and 4 we can be certain that the whole purification procedure went well without losing any protein. Nevertheless, it is no surprise that the constructs failed to purify. It has been previously noted that even one amino acid change can destabilize the entire protein (Babon et al. 2014). Here we had six amino acids change and a bulky fluorescent protein attached to either sides of JAK2 JH2-JH1 domains. While designing the constructs the sites of structural divergence among typical tyrosine kinases were identified for insertion of the tetracysteine motif. Such divergence was thought to presumably exert no particular effect on the structure and function of the proteins. By looking at Figure 6 it is evident that the constructs are expressed in mammalian cells meaning that it is the protein production conditions that need optimizing to achieve protein yields. Temperature as well as incubation time of insect cells with the virus can be varied between 22 to 27 ºC and between 48 to 72-hours incubation time. The concentration of

virus during infection can also play a role in protein production, therefore testing the production at 1, 5 and 10% virus could bring a different outcome. When attempting to purify and crystalize JAKs it is common to create kinase inactive mutants by introducing a kinase inactivating mutation (as D1023N in TYK2) that confers a more stable protein (Lupardus et al. 2014). Furthermore, introduction of tetracysteine motif could have exposed some hydrophobic residues that caused insolubility of the constructs. Our JH2-JH1 sequence started at 536 valine residue, yet it is also common that JH2-JH1 experimental constructs are longer and start at 513 residue.

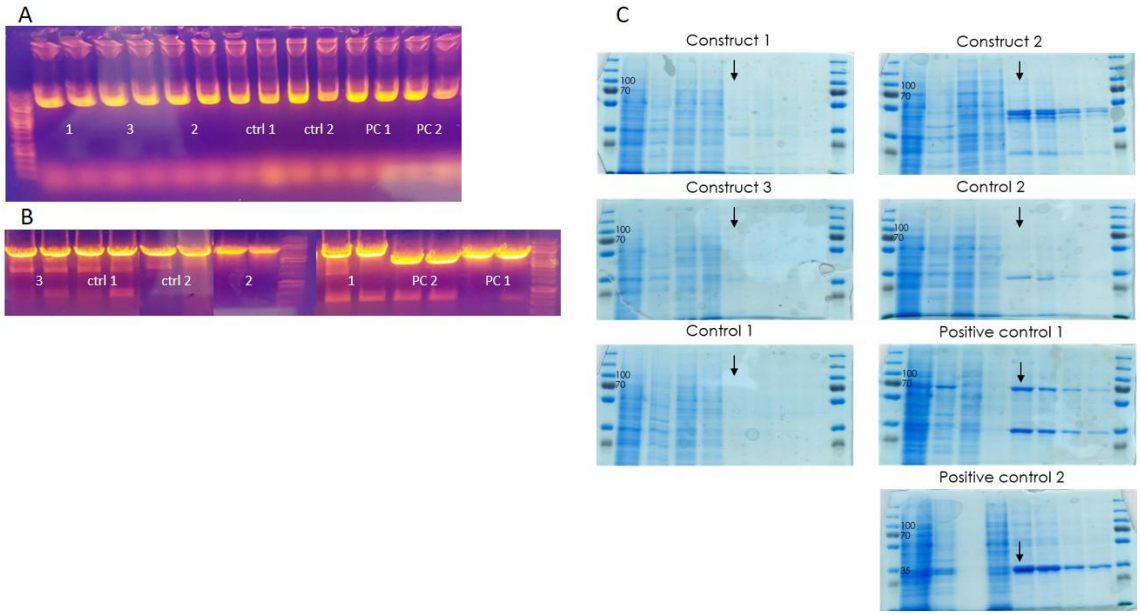


***Figure 7.*** *A) Agarose gel analysis of transposed bacmids helper plasmid and RNA contamination levels. B) PCR verification of Bacmid transposition. The size of construct of interest is 4800 bb, the size of positive controls 1 and 2 is 4100 and 3200 bp, respectively. C) SDS-PAGE gels of purified constructs. The construct molecular weight is 100 kDa, the molecular weight of positive control 1 and 2 is 70 and 35 kDa, respectively. The positions of purified protein bands are marked with black arrows.*

## 3.3 FRET

### 3.3.1 Time lapse imaging

In this study, we considered two ways of examining energy transfer between fluorophores. The first method is direct monitoring of decrease in donor fluorescence intensity upon addition of the acceptor fluorophore. This method was described by Hoffmann et al. (2010) who observed an up to 50% decrease in CFP fluorescence intensity after the addition of FlAsH-EDT2 in their constructs. Time series imaging was performed for one hour with 3-minutes intervals between capturing. Testing of this method was implemented only for constructs 1 and 2 and was aborted due to technical limitations,

however the results are presented below in Figure 8. In Figure 8, A and B the fluorescence intensity between constructs 1 and 2 and corresponding controls is presented. The graphs demonstrate that the CFP fluorescence intensity in constructs containing FlAsH-binding motif starts to reduce right after the addition of the fluorescent dye. This is an anticipated event that indicates an occurrence of FRET between CFP and FLAsH-EDT2. Construct 2 shows greater than 50% change in the CFP intensity, whereas construct 1 displays a 20% reduction after which it returns to the original state and doesn't change anymore. Both controls, on the other hand, demonstrate a regular increase in donor intensity, being a mere 20% change in control 1 and remarkable 100% change in control 2. These changes, however, are not attributes of any biological or physical processes of energy transfer that we were aiming to see. These changes occurred due to the imperfect focus system of the microscope that failed to keep the sample continuously in focus during time-lapse imaging. When left alone the shifting of focus caused the entire image to dim leading to seeming quenching of CFP fluorescence intensity as in construct 2. When the time series imaging was interrupted and the focus adjusted back to being sharp and crisp, the donor fluorescence intensity returned back to being around the initial values as in construct 1 after the eighth cycle. Another factor contributing to loss of focus is cell movement within the scanning z-plane and migration between the planes. The latter reason in particular caused troubles in continuous measurements of CFP fluorescence since not every cell in the chosen area was fluorescent. Therefore, migration of CFP expressing cells resulted in 'reduced' CFP fluorescent intensity of the whole area. Unfortunately, this issue can only be addressed by using more complicated instrumentation since fixing cells will not anymore allow proper labeling. Coincidentally, an opposite effect of loss of focus was observed in both controls. In case of control 2 the focus was disturbed right after the addition of the label, but was adjusted after the second cycle after which the CFP fluorescence intensity fluctuated at around 2.

Even though this method did not yield any useful results it allowed optimization of the labeling and washing procedures. The suitable incubation time with FlAsH-EDT2 could be identified. The time length depended on the position of the fluorescent tag motif, being longer for the constructs that harbored the tag in their interior loops. The saturation of FlAsH fluorescence, for instance, was observed quicker in construct 1 in comparison to construct 2 or 3, due to the terminal location of the tag, which allows for easy access by fluorescent dye. In Figure 8, C and D, the representative images of labeled cells after 1 – 1.5-hours incubation and before washing are presented. Once the desired fluorescence was reached the cells were subjected to washing with 1,2-ethanedithiol, an antidot for FlAsH-EDT2. Because FlAsH-EDT2 has a tendency to bind unspecifically to cysteine rich proteins as well as within hydrophobic protein compartments, addition of excess amounts of dithiols binds the unbound and loosely bound bisarsenic compounds. As it can be seen in images of FlAsH-EDT2 after wash and with only CFP, the FlAsH fluorescence of CFP expressing cells is higher than in the surrounding untransfected cells. In the controls, however, the FlAsH-EDT2 intensity after washing is uni-

form among untransfected and transfected, CFP expressing cells. This demonstrates that we achieved specific labelling of tetracysteine tag.

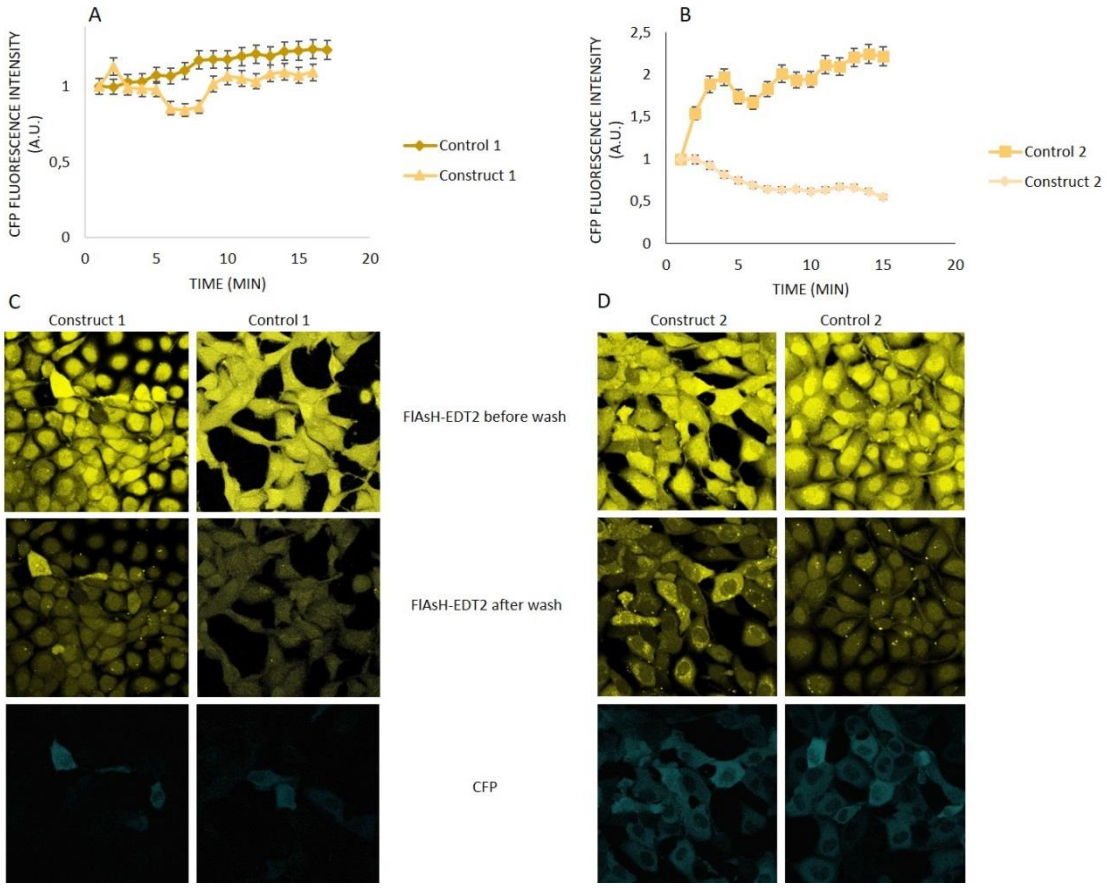


***Figure 8.*** *A) and B) Time lapse measurements of CFP fluorescence intensity. The measurements were performed over 15 cycles of 3 minutes by monitoring the intensity of FRET donor. The results are normalized to the first value after subtraction of background signal and presented with standard error. C) and D) Representative images of specificity of labeling with FlAsH-EDT2. The cells exhibited saturation in 514-565 nm channel (FlAsH channel) after 1-1.5h of incubation with FlAsH-EDT2. The unspecific binding was reduced by a washing step with 1,2-ethanedithiol (EDT). The turquoise fluorescent cells in the lowest row of construct 1 and 2 contain a tetracysteine biding motif, whereas the controls do not. The presence of tetracysteine binding motif confers a considerably brighter yellow fluorescence indicative of specific labeling.*

### 3.3.2 FRET by acceptor photobleaching

Acceptor photobleaching is a popular FRET approach for qualitative evaluation of biological processes on as small as under 10 nm scale. It is a relatively straightforward way to analyze stable as well as transient protein-protein interactions. Here, we analyzed FRET efficiency by carrying out measurements of donor fluorescence recovery after acceptor photobleaching in CFP – FlAsH-EDT2 FRET pair. The results are a mean of three independent experiments per construct, each performed on 20-30 cells. Cells with

approximately equal CFP-expression levels were selected to facilitate a comparative analysis. The t- and p-values of FRET efficiency between +/- VF constructs are presented in figures 9 and 10 with degrees of freedom shown in brackets. The p-value of FRET efficiency difference between the constructs and their corresponding controls was < 0.001 in every situation. FRET efficiency measurements by acceptor photobleaching were carried out in both, live and fixed cells. Live cells measurements were performed under physiological conditions in 5% $CO_2$ air at 37ºC.

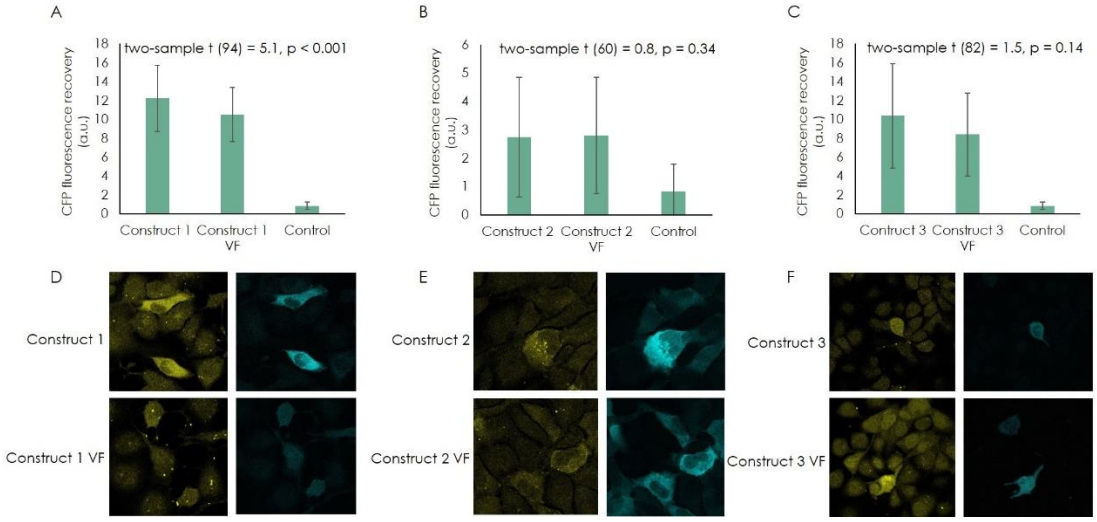


***Figure 9.*** *FRET efficiency by acceptor photobleaching in intact cells. A) Construct 1 +/- VF, B) construct 2 +/- VF, C) construct 3 +/- VF. The t- and p-values are obtained with two-sample t-test and presented for constructs with and without VF mutation. The significance of FRET efficiency difference between constructs and controls is more than 99.9%. D), E) and F) representative images of labeling specificity with FlAsH-EDT2.*

Figure 9, A, B and C demonstrate the FRET efficiency of constructs 1, 2 and 3 with and without V617F mutation and the corresponding controls in living cells. Figure 9, D, E and F contain representative images of labelled cells depicting specific binding of FlAsH to tetracysteine regions. The FRET efficiency is presented as efficiency of recovery of fluorescence intensity of the donor after photobleaching of the acceptor in a selected ROI of arbitrary size. It is evident that donor fluorescence recovery is significantly higher (p-value < 0.001) in constructs containing tetracysteine sequence in comparison to controls, which means that FRET between CFP and FlAsH-EDT2 indeed takes place in our constructs. The difference in FRET efficiency between constructs with and without VF, however, is statistically significant only in construct 1 with p-value < 0.001. Construct 1 VF exhibits lower FRET efficiency, which implies that introduction of VF mutation causes the distance separating two fluorophores to increase. No significant changes of FRET efficiency between +/- VF in constructs 2 and 3 was observed indicating no considerable effect of this mutation to the interior of our protein of interest. It can be noticed, however, that the standard deviation of FRET efficiency in cells transfected with constructs 2 and 3 +/- VF is markedly large. This can be explained

by the fact, that despite strict adherence to standardized protocol for labeling with FlAsH-EDT2 it was not always possible to achieve equal labeling intensity on different days. The labelling intensity was compared by calculating CFP/FlAsH-EDT2 intensity ratio. The reason for such variations is still unclear since no deviations from optimal concentrations of reagents, DNA or number of seeded cells occurred. To overcome this issue, it was decided to conduct FRET efficiency measurements in fixed cells that were labeled and fixed simultaneously on the same day. Another modification to our experimental setup was to carry out whole cell photobleaching rather than of a specific region of interest. It caught our attention that photobleaching of a selected ROI resulted in immediate attenuation of FRET following the first cycle after acceptor photobleaching. FRET attenuation can be attributed to diffusion of probe bound POI to the ROI that results in quenching of donor fluorescence (Karpova et al. 2003). It is worth pointing out that the immediate change was always higher between the fifth and sixth cycles (right before and right after bleaching) than the mean of five cycles before and after bleaching. Bleaching of the whole cell was deemed to prevent such problem and show a more stable donor fluorescence recovery. If this problem would not be eliminated disappearance of FRET in the cycles following bleaching could have a certain different meaning (Karpova and McNally 2006).

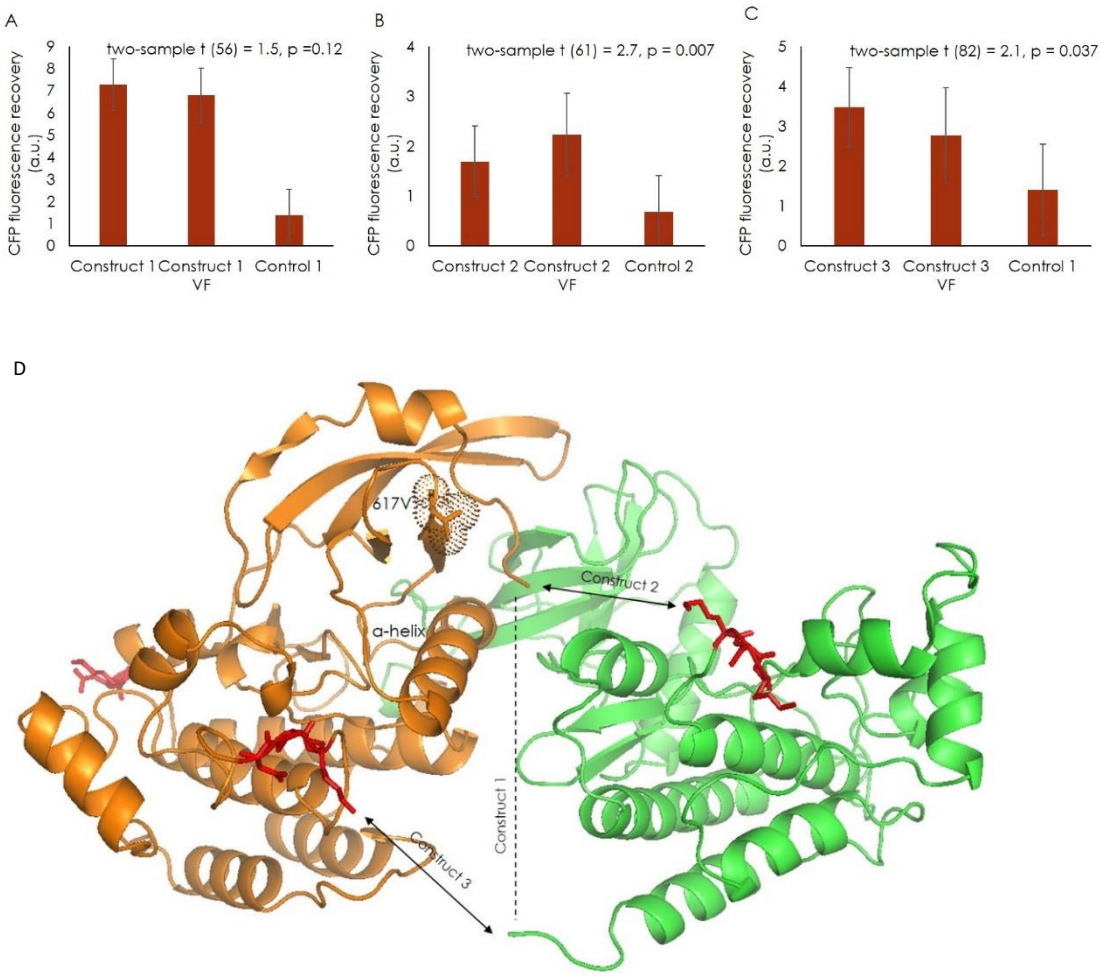


***Figure 10.*** *FRET efficiency by acceptor photobleaching in fixed cells. A) Construct 1 +/- VF, B) construct 2 +/- VF, C) construct 3 +/- VF. The t- and p-values are obtained with two-sample t-test and presented for constructs with and without VF mutation. The significance of FRET efficiency difference between constructs and controls is more than 99.9%. D) A cartoon representation of JAK2 JH2 (in orange) and JH1 (in green) domains with tetracysteine motives highlighted in red, V617 enclosed in transparent spheres and interactions of fluorophores in every construct are indicated by arrows.*

Figure 10, A, B and C present the results of FRET efficiency measurements by acceptor photobleaching in fixed cells. It can be seen that by implementing measurements in fixed cells we were able to achieve a reduction in the measurement deviation among samples. The average labelling intensities between the constructs with and without V617F mutation were also comparable being 0.72 and 0.71 for construct 1 +/- VF, 1.86 and 1.84 for construct 2 +/- VF and 0.80 and 0.71 for construct 3 +/- VF. It might be noticed, though, that the overall signal of CFP fluorescence is lower in fixed cells, yet we still observe a significant difference (p-value < 0.001) between constructs with tetracysteine motif and controls without thereof. The change in FRET efficiency in construct 1 with VF is now, however, almost indistinguishable from construct 1 without VF with only 88% confidence level of FRET efficiency decrease. Even though this result contra-

dicts what we observed in intact cells such outcome could be anticipated due to several reasons. Most importantly, it should be pointed out that in construct 1 the fluorophores are attached through short, but still quite flexible linkers. Such flexibility allows easy reorientation of the fluorophores and even if a small conformational change occurred inside the protein the effect would not necessarily be prominent. Such flexibility, on the other hand, leads to comparatively higher overall FRET efficiency than in constructs 2 and 3. This can be attributed to higher probability of correct positioning of transitional dipoles of two fluorophores. Nevertheless, statistically significant change in FRET efficiency can now be recognized in constructs 2 and 3 between wild type and V617F mutation. An increase in FRET efficiency is detected (p-value = 0.007) in construct 2 with VF indicating that introduction of comparably large phenylalanine residue results in distance reduction by 0.54. Construct 3 VF, on the contrary, demonstrates a decrease in FRET efficiency (p-value = 0.037) by 0.71 implying a reverse effect on separation distance.

Despite seemingly complicated outcome of this study, our results can be interpreted in a reasonable way. Figure 10, D illustrates how mutation of 617 valine to phenylalanine (highlighted by transparent spheres) induces a conformational change between JH2 and JH1 domains in JAK2. The representation of interdomain interactions in Figure 10, D is of course not precise since CFP is missing from the picture, but it gives a relative understanding of occurring alterations. It can be seen that the increase in distance between the C-terminus of JH1 and 726-728 residues of JH2 can lead to the decrease in distance between the N-terminus of JH2 and residues 1053-1055 due to their positioning opposite to each other. The conformational change induced by V617F mutation in construct 2 directs the N-lobe of JH2 domain towards the hinge region in JH1 presumably affecting its entire catalytic site. Activation of JAKs is underlined by expulsion of activation loop from the catalytic site. Therefore, the hyperactivatory effect of V617F mutation can be associated with rotation of JH2 N-lobe towards the catalytic loop in JH1 resulting in physical expulsion of A-loop and exposure of Y1007 and Y1008 for phosphorylation. Our finding plays an important role in trying to decipher how mutation of one amino acid leads to non-stop activity of such crucial enzyme in organismal homeostasis as JAK2.

# 4. DISCUSSION

Protein-protein interaction studies have been performed *in vitro* with isolated proteins now for many years (Dwane and Kiely 2011). The method is advantageous in many terms. For instance, controlled protein concentration and, hence, peptide tag concentration, sensitivity of measuring devices that can detect even the weakest interactions and independence of expression levels unlike in cell experiments (Phizicky and Fields 1995). However, due to difficulty of isolation of certain proteins and their insolubility (Karpova and McNally 2006), the *in vitro* approach is at times unavailable. To overcome this issues the fluorescence resonance energy transfer approach in cells is capable of detecting protein-protein interactions on the 10 nm scale (Karpova and McNally 2006; Vaiyapuri et al. 2015; Abraham 2015). FRET is based on the intrinsic properties of a fluorophore in an excited state to transfer some of its energy to another fluorophore provided sufficient spectrum overlap (Abraham et al. 2011). Traditionally different variants of green fluorescence proteins were used in FRET analysis, however due to their large molecular weight (approximately 27 kDa) these fluorescent markers can alter the functionality and native structure of the target protein (Adams et al. 2002; Hoffmann et al. 2010). In the first paper reporting CFP-FlasH based FRET (Hoffmann et al. 2005) it was demonstrated that use of YFP-CFP FRET pair via insertion of YFP to an intracellular loop of $A_{2A}$-adenosine receptor in addition to CFP at the C-terminus of the receptor completely perturbed the signaling function of the protein. To tackle this issue genetically encoded tags in conjunction with small fluorescent molecule dyes were invented that can replace the use of cumbersome fluorescent proteins and allow the study of nearly unchanged proteins (Soh 2008).

There exist several methods to FRET measurements, each with its own advantages. While FRET by lifetime imaging enables the most accurate analysis, FRET steady state measurements by acceptor photobleaching is a widely-accepted technique due to its straightforward nature (Karpova and McNally 2006; Abraham 2015). With an easy set-up, as in our study, it allows visualization of a few nanometer changes in protein conformation. With a more vigorous system the changes can be assessed quantitatively providing invaluable knowledge of spatial transposition and localization of biomolecules of interest. Despite the requirements for excessive controls for normalization and calibration such system helps to achieve quantification of relevant FRET efficiency and separation distances (Karpova et al. 2003; Karpova and McNally 2006; Zal and Gascoigne 2004). In our study, we implement a simpler approach to analysis of the orientational changes between pseudokinase and kinase domains of JAK2 in wild type and under a function disruptive mutation. The mutation of interest in this work is V617F

which was identified as a major cause for 95% of polycythemia vera incidences and 60% of essential thrombocythemia (Hammarén et al. 2015; Klampfl et al. 2013). Due to an effect of so called allele burden addressing the disorders caused by V617F mutation as early as possible is crucial to prevent its progression into more severe diseases that eventually lead to leukemia (Passamonti and Rumi 2009).

Here, we demonstrated a conformational change induced by the introduction of V617F mutation in the studied constructs. Phenylalanine is a considerably large amino acid that has previously been shown to modify the α-helix in the N-lobe of JH2 domain (Bandaranayake et al. 2012). In particular, the replacement of valine at 617 by phenylalanine resulted in rigidification of α-helix due to attractive aromatic interactions of three phenylalanines at 594, 595 and 617 positions. Moreover, the α-helix was found to be extended by a turn at its amino-terminus which is proximal to the N-lobe of JH1 (Bandaranayake et al. 2012). Our results complement these findings by showing that V617F mutation causes the N-lobe of JH2 to turn towards the hinge region in JH1 by juxtaposing the N-terminus of JH2 to the insertion loop of JH1. Such change is accompanied by separation of the C-terminus of JH1 from the 726-728 residues in the C-lobe of JH2. It is possible that this conformational change has an influence on the catalytic site of JH1 domain resulting in constitutive activation of JAK2. Furthermore, in earlier studies, insertion loop of kinase domain was identified to exert a unique function in JAK kinases and recognized as a possible regulator of autophosphorylation activity and interdomain interaction with FERM domain (Boggon et al. 2005; Lucet et al. 2006). By placing a tetracysteine tag at position 1053-1055, right before the start of the insertion loop of JAK2 kinase domain, we observed a positional shift in this important regulatory site.

Further investigation of this subject is required to unravel more exact structural alterations imposed by V617F mutation. Using the system established through this work as a foundation it is possible to resolve other unexplored questions. For instance, our concept could be strengthened by observing the results of reversing the effect of V617F mutation using JAK2 inhibitors, such as ruxolitinib (Kogan et al. 2015), or by introduction of kinase deactivating mutation. While these methods will not necessarily demonstrate the same levels of FRET efficiency as in our wild type constructs they might help realize what is essential for disruption of suppressory effect of JH2 on JH1 domain caused by V617F mutation. The simple site-directed mutagenesis procedure can be used to insert the tetracysteine tag into other locations of our protein of interest. In fact, when the tetracysteine tag system was first developed by Griffin et al (1998) they embedded the four cysteines at the i, i+1, i+4, and i+5 loci of a helix to create a parallelogram that could perfectly bind FlAsH-EDT2. Such approach can be implemented to see how the position of α-helix in JH2 changes in pathogenic constructs.

To further advance our knowledge in this matter, the same approach can be used in full-length JAK2 and by generating stably transfected cell lines to avoid the overexpression

of protein in transient transfection and to reduce toxicity. Using full-length protein constructs would also allow to ensure the unperturbed kinase activity of JAK2 after introduction of the tetracysteine motif and fusion with FPs. Presence of the FERM and SH2 domains responsible for receptor association would enable monitoring of receptor and STAT phosphorylation (Chrencik et al. 2010; Yamaoka et al. 2004). With the current experimental setup, it is unclear whether the function of JH2-JH1 domains was disturbed by addition of fluorescent tags. To our surprise, we observed no phosphorylation of 1007 and 1008 tyrosines in VF constructs 1 and 3. On the other hand, the construct 2 without VF appeared phosphorylated implying less inhibitory interactions between JH2 and JH1. Such effect could be observed due to our specific construct design. Nevertheless, it can be concluded that such phosphorylation patterns are caused by addition of CFP and independent of tetracysteine tag since similar effect was detected in controls 1 and 2 that did not possess FlAsH binding site. Notwithstanding this fact, our results are still comparable because phosphorylation levels are the same in wild type and corresponding VF constructs but we do once again encounter the issue of FPs inconvenient size. To overcome this problem, a different approach can be utilized that evades involvement of FPs. FlAsH-EDT2 and his-tag labelled by Ni-NTA conjugated fluorescent reporters has been successfully shown as a donor-acceptor pair in FRET measurements (Krishnan, Szymanska, and Gierasch 2007). As a drawback, fluorescent labeling of his-tag results in undesired amounts of unspecific binding (Christian R. Goldsmith et al. 2005; Lata et al. 2006), however the protein-protein interactions could be differentiated by FRET. To further ensure that the measured cells are actually transfected another fluorescent reporter with emission somewhere in infra-red spectrum could be added that would not overlap the excitation/emission spectrum of FRET pair fluorescent labels.

# 5. CONCLUSION

Using a FRET based approach to investigation of interdomain interactions and conformational dynamics of JAK2 pseudokinase and kinase domains we identified novel changes induced by V617F mutation to JAK2 wild type structure. We revealed that mutation of 617-valine to phenylalanine leads to reorientation of JH2 N-lobe towards the catalytic site of kinase domain thereby increasing the distance between the C-terminus of JH1 and the 726-728 residues in the C-lobe of JH2. We believe that such changes can underlie the hyperactivatory effect of V617F mutation that disrupts the basal inhibition of catalytic domain by pseudokinase domain. Further studies could shed more light onto the detrimental effect of V617F mutation enabling development of mutant-specific, more efficacious pharmaceutical agents.

# REFERENCES


Abraham, Bobin George. 2015. *Fluorescent Protein Toolbox: Protein Engineering Broadens the Range of in Vitro and in Vivo Applications of Fluorescent Proteins.* Tampere: Tampere University of Technology.

Abraham, Bobin George, Nikolai V. Tkachenko, Ville Santala, Helge Lemmetyinen, and Matti Karp. 2011. "Bidirectional Fluorescence Resonance Energy Transfer (FRET) in Mutated and Chemically Modified Yellow Fluorescent Protein (YFP)." *Bioconjugate Chemistry* 22(2):227–34. Retrieved April 2, 2017 (http://www.ncbi.nlm.nih.gov/pubmed/21275395).

Adams, Stephen R. et al. 2002. "New Biarsenical Ligands and Tetracysteine Motifs for Protein Labeling in Vitro and in Vivo: Synthesis and Biological Applications." *Journal of the American Chemical Society* 124(21):6063–76. Retrieved April 2, 2017 (http://www.ncbi.nlm.nih.gov/pubmed/12022841).

Babon, Jeffrey J., Isabelle S. Lucet, James M. Murphy, Nicos A. Nicola, and Leila N. Varghese. 2014. "The Molecular Regulation of Janus Kinase (JAK) Activation." *The Biochemical Journal* 462(1):1–13. Retrieved December 19, 2016 (http://www.ncbi.nlm.nih.gov/pubmed/25057888).

Bandaranayake, Rajintha M. et al. 2012. "Crystal Structures of the JAK2 Pseudokinase Domain and the Pathogenic Mutant V617F." *Nature Structural & Molecular Biology* 19(8):754–59. Retrieved January 19, 2017 (http://www.ncbi.nlm.nih.gov/pubmed/22820988).

Barry, G. F. 1988. "A Broad-Host-Range Shuttle System for Gene Insertion into the Chromosomes of Gram-Negative Bacteria." *Gene* 71(1):75–84. Retrieved April 17, 2017 (http://www.ncbi.nlm.nih.gov/pubmed/2850977).

Berney, Claude and Gaudenz Danuser. 2003. "FRET or No FRET: A Quantitative Comparison." *Biophysical Journal* 84(6):3992–4010. Retrieved April 26, 2017 (http://www.ncbi.nlm.nih.gov/pubmed/12770904).

Bhunia, Anjan K. and Stephen C. Miller. 2007. "Labeling Tetracysteine-Tagged Proteins with a SplAsH of Color: A Modular Approach to Bis-Arsenical Fluorophores." *ChemBioChem* 8(14):1642–45. Retrieved April 25, 2017 (http://doi.wiley.com/10.1002/cbic.200700192).

Boggon, T. J., Yiqun Li, Paul W. Manley, and Michael J. Eck. 2005. "Crystal Structure of the Jak3 Kinase Domain in Complex with a Staurosporine Analog." *Blood* 106(3):996–1002. Retrieved March 3, 2017 (http://www.ncbi.nlm.nih.gov/pubmed/15831699).

Brooks, A. J. et al. 2014. "Mechanism of Activation of Protein Kinase JAK2 by the

Growth Hormone Receptor." *Science* 344(6185):1249783–1249783. Retrieved March 9, 2017 (http://www.ncbi.nlm.nih.gov/pubmed/24833397).

Bäumle, Monika et al. n.d. "Nitrilotriacetate-Atto Dye Conjugates For The Fluorescence Detection Of Oligo-Histidine Tagged Proteins Characterization of the Chromophore-NTA Conjugate." 5–6.

Chen, Baowei, Haishi Cao, Ping Yan, M.Uljana Mayer, and Thomas C. Squier. 2007. "Identification of an Orthogonal Peptide Binding Motif for Biarsenical Multiuse Affinity Probes." *Bioconjugate Chemistry* 18(4):1259–65. Retrieved April 25, 2017 (http://www.ncbi.nlm.nih.gov/pubmed/17569496).

Chen, Edwin, Louis M. Staudt, and Anthony R. Green. 2012. "Janus Kinase Deregulation in Leukemia and Lymphoma." *Immunity* 36(4):529–41. Retrieved March 2, 2017 (http://www.ncbi.nlm.nih.gov/pubmed/22520846).

Chrencik, Jill E. et al. 2010. "Structural and Thermodynamic Characterization of the TYK2 and JAK3 Kinase Domains in Complex with CP-690550 and CMP-6." *Journal of Molecular Biology* 400(3):413–33.

Christian R. Goldsmith, †, ‡ Jacek Jaworski, ‡,§ and Morgan Sheng, and † Stephen J. Lippard*. 2005. "Selective Labeling of Extracellular Proteins Containing Polyhistidine Sequences by a Fluorescein−Nitrilotriacetic Acid Conjugate." Retrieved May 21, 2017 (http://pubs.acs.org/doi/abs/10.1021/ja0559754).

Chudakov, Dmitriy M., Mikhail V. Matz, Sergey Lukyanov, and Konstantin A. Lukyanov. 2010. "Fluorescent Proteins and Their Applications in Imaging Living Cells and Tissues." *Physiological Reviews* 90(3). Retrieved April 23, 2017 (http://physrev.physiology.org/content/90/3/1103.long).

Crone, Donna E. et al. 2013. "GFP-Based Biosensors." *State of the Art in Biosensors - General Aspects*. Retrieved May 21, 2017 (http://www.bioinfo.rpi.edu/bystrc/pub/crone_etal.pdf).

Deininger, Michael et al. 2015. "The Effect of Long-Term Ruxolitinib Treatment on JAK2p.V617F Allele Burden in Patients with Myelofibrosis." *Blood* 126(13). Retrieved April 22, 2017 (http://www.bloodjournal.org/content/126/13/1551?sso-checked=true).

Donna et al. 2013. "GFP-Based Biosensors." in *State of the Art in Biosensors - General Aspects*. InTech. Retrieved April 23, 2017 (http://www.intechopen.com/books/state-of-the-art-in-biosensors-general-aspects/gfp-based-biosensors).

Duhé, Roy J., Emily A. Clark, and William L. Farrar. 2002. "Characterization of the in Vitro Kinase Activity of a Partially Purified Soluble GST/JAK2 Fusion Protein." *Molecular and Cellular Biochemistry* 236(1–2):23–35. Retrieved January 13, 2017 (http://www.ncbi.nlm.nih.gov/pubmed/12190118).

Dusa, Alexandra, Céline Mouton, Christian Pecquet, Murielle Herman, and Stefan N. Constantinescu. 2010. "JAK2 V617F Constitutive Activation Requires JH2 Residue F595: A Pseudokinase Domain Target for Specific Inhibitors" edited by

A. M. Delprato. *PLoS ONE* 5(6):e11157. Retrieved March 5, 2017 (http://www.ncbi.nlm.nih.gov/pubmed/20585391).

Dwane, Susan and Patrick A. Kiely. 2011. "Tools Used to Study How Protein Complexes Are Assembled in Signaling Cascades." *Bioengineered Bugs* 2(5):247–59. Retrieved May 21, 2017 (http://www.ncbi.nlm.nih.gov/pubmed/22002082).

Finbloom, D. S. and A. C. Larner. 1995. "Regulation of the Jak/STAT Signalling Pathway." *Cellular Signalling* 7(8):739–45. Retrieved December 19, 2016 (http://www.ncbi.nlm.nih.gov/pubmed/8593242).

Gautier, Arnaud et al. 2008. "An Engineered Protein Tag for Multiprotein Labeling in Living Cells." *Chemistry & Biology* 15(2):128–36. Retrieved April 2, 2017 (http://www.ncbi.nlm.nih.gov/pubmed/18291317).

Ghoreschi, K. et al. 2011. "Modulation of Innate and Adaptive Immune Responses by Tofacitinib (CP-690,550)." *The Journal of Immunology* 186(7):4234–43. Retrieved March 24, 2017 (http://www.ncbi.nlm.nih.gov/pubmed/21383241).

Giordanetto, Fabrizio and Romano T. Kroemer. 2002. "Prediction of the Structure of Human Janus Kinase 2 (JAK2) Comprising JAK Homology Domains 1 through 7." *Protein Engineering* 15(9):727–37. Retrieved December 22, 2016 (http://www.ncbi.nlm.nih.gov/pubmed/12456871).

Goedhart, Joachim et al. 2010. "Bright Cyan Fluorescent Protein Variants Identified by Fluorescence Lifetime Screening." *Nature Methods* 7(2):137–39. Retrieved April 2, 2017 (http://www.nature.com/doifinder/10.1038/nmeth.1415).

Griffin, B. A., S. R. Adams, and R. Y. Tsien. 1998. "Specific Covalent Labeling of Recombinant Protein Molecules inside Live Cells." *Science (New York, N.Y.)* 281(5374):269–72. Retrieved April 2, 2017 (http://www.ncbi.nlm.nih.gov/pubmed/9657724).

Gu, Y., W. L. Di, D. P. Kelsell, and D. Zicha. 2004. "Quantitative Fluorescence Resonance Energy Transfer (FRET) Measurement with Acceptor Photobleaching and Spectral Unmixing." *Journal of Microscopy* 215(2):162–73. Retrieved April 2, 2017 (http://www.ncbi.nlm.nih.gov/pubmed/15315503).

Haishi Cao et al. 2007. "A Red Cy3-Based Biarsenical Fluorescent Probe Targeted to a Complementary Binding Peptide." Retrieved April 24, 2017 (http://pubs.acs.org/doi/abs/10.1021/ja070003c).

Haleem J. Rasool. 2016. "Myeloproliferative Disease: Practice Essentials, Background, Pathophysiology." *Medscape*. Retrieved December 22, 2016 (http://emedicine.medscape.com/article/204714-overview).

Hammarén, Henrik M. et al. 2015. "ATP Binding to the Pseudokinase Domain of JAK2 Is Critical for Pathogenic Activation." *Proceedings of the National Academy of Sciences* 112(15):4642–47. Retrieved December 22, 2016 (http://www.ncbi.nlm.nih.gov/pubmed/25825724).

Heim, Roger, Andrew B. Cubitt, and Roger Y. Tsien. 1995. "Improved Green

Fluorescence." *Nature* 373(6516):663–64. Retrieved April 23, 2017 (http://www.ncbi.nlm.nih.gov/pubmed/7854443).

Hoffmann, Carsten et al. 2005. "A FlAsH-Based FRET Approach to Determine G Protein–coupled Receptor Activation in Living Cells." *Nature Methods* 2(3):171–76. Retrieved April 2, 2017 (http://www.ncbi.nlm.nih.gov/pubmed/15782185).

Hoffmann, Carsten et al. 2010. "Fluorescent Labeling of Tetracysteine-Tagged Proteins in Intact Cells." *Nature Protocols* 5(10):1666–77. Retrieved January 11, 2017 (http://www.ncbi.nlm.nih.gov/pubmed/20885379).

Hussain, Syed Arshad. 2008. "An Introduction to Fluorescence Resonance Energy Transfer (FRET)." Retrieved April 25, 2017 (https://arxiv.org/ftp/arxiv/papers/0908/0908.1815.pdf).

Johnsson, K. et al. 2011. "NCCR ChemiCal Biology Visualizing Biochemical Activities in Living Cells through Chemistry." *Chimia* 65:868–71. Retrieved April 24, 2017 (http://www.ingentaconnect.com/content/scs/chimia/2011/00000065/00000011/art00010?crawler=true).

Karpova, T. S. et al. 2003. "Fluorescence Resonance Energy Transfer from Cyan to Yellow Fluorescent Protein Detected by Acceptor Photobleaching Using Confocal Microscopy and a Single Laser." *Journal of Microscopy* 209(Pt 1):56–70. Retrieved May 22, 2017 (http://www.ncbi.nlm.nih.gov/pubmed/12535185).

Karpova, Tatiana and James G. McNally. 2006. "Detecting Protein-Protein Interactions with CFP-YFP FRET by Acceptor Photobleaching." P. Unit12.7 in *Current Protocols in Cytometry*, vol. Chapter 12. Hoboken, NJ, USA: John Wiley & Sons, Inc. Retrieved April 2, 2017 (http://www.ncbi.nlm.nih.gov/pubmed/18770833).

Keppler, Antje et al. 2002. "A General Method for the Covalent Labeling of Fusion Proteins with Small Molecules in Vivo." *Nature Biotechnology* 21(1):86–89. Retrieved April 24, 2017 (http://www.ncbi.nlm.nih.gov/pubmed/12469133).

Keppler, Antje, Claudio Arrivoli, Lucia Sironi, and Jan Ellenberg. 2006. "Fluorophores for Live Cell Imaging of AGT Fusion Proteins across the Visible Spectrum." *BioTechniques* 41(2):167–70, 172, 174–75. Retrieved April 24, 2017 (http://www.ncbi.nlm.nih.gov/pubmed/16925018).

Kishimoto, T., T. Taga, and S. Akira. 1994. "Cytokine Signal Transduction." *Cell* 76(2):253–62. Retrieved December 20, 2016 (http://www.ncbi.nlm.nih.gov/pubmed/8293462).

Klampfl, Thorsten et al. 2013. "Somatic Mutations of Calreticulin in Myeloproliferative Neoplasms." *New England Journal of Medicine* 369(25):2379–90. Retrieved March 1, 2017 (http://www.nejm.org/doi/abs/10.1056/NEJMoa1311347).

Kogan, I. et al. 2015. "JAK-2 V617F Mutation Increases Heparanase Procoagulant Activity." *Thrombosis and Haemostasis* 115(1):73–80. Retrieved May 16, 2017 (http://www.ncbi.nlm.nih.gov/pubmed/26489695).

Kohlhuber, F. et al. 1997. "A JAK1/JAK2 Chimera Can Sustain Alpha and Gamma

Interferon Responses." *Molecular and Cellular Biology* 17(2):695–706. Retrieved January 16, 2017 (http://www.ncbi.nlm.nih.gov/pubmed/9001223).

Kontzias, Apostolos, Alexander Kotlyar, Arian Laurence, Paul Changelian, and John J. O'Shea. 2012. "Jakinibs: A New Class of Kinase Inhibitors in Cancer and Autoimmune Disease." *Current Opinion in Pharmacology* 12(4):464–70. Retrieved March 24, 2017 (http://www.ncbi.nlm.nih.gov/pubmed/22819198).

Krishnan, Beena, Aneta Szymanska, and Lila M. Gierasch. 2007. "Site-Specific Fluorescent Labeling of Poly-Histidine Sequences Using a Metal-Chelating Cysteine." *Chemical Biology & Drug Design* 69(1):31–40. Retrieved May 16, 2017 (http://www.ncbi.nlm.nih.gov/pubmed/17313455).

Lang, Kathrin and Jason W. Chin. 2014. "Cellular Incorporation of Unnatural Amino Acids and Bioorthogonal Labeling of Proteins."

Lata, Suman et al. 2006. "Specific and Stable Fluorescence Labeling of Histidine-Tagged Proteins for Dissecting Multi-Protein Complex Formation." (21):2365–72.

Los, Georgyi V. et al. 2008. "HaloTag: A Novel Protein Labeling Technology for Cell Imaging and Protein Analysis." *ACS Chemical Biology* 3(6):373–82. Retrieved April 23, 2017 (http://pubs.acs.org/doi/abs/10.1021/cb800025k).

Lucet, I. S. et al. 2006. "The Structural Basis of Janus Kinase 2 Inhibition by a Potent and Specific Pan-Janus Kinase Inhibitor." *Blood* 107(1):176–83. Retrieved January 19, 2017 (http://www.ncbi.nlm.nih.gov/pubmed/16174768).

Lukyanov, Konstantin A., Dmitry M. Chudakov, Sergey Lukyanov, and Vladislav V. Verkhusha. 2005. "Innovation: Photoactivatable Fluorescent Proteins." *Nature Reviews Molecular Cell Biology* 6(11):885–90. Retrieved April 23, 2017 (http://www.nature.com/doifinder/10.1038/nrm1741).

Luo, H. et al. 1997. "Mutation in the Jak Kinase JH2 Domain Hyperactivates Drosophila and Mammalian Jak-Stat Pathways." *Molecular and Cellular Biology* 17(3):1562–71. Retrieved January 16, 2017 (http://www.ncbi.nlm.nih.gov/pubmed/9032284).

Lupardus, P. J. et al. 2014. "Structure of the Pseudokinase-Kinase Domains from Protein Kinase TYK2 Reveals a Mechanism for Janus Kinase (JAK) Autoinhibition." *Proceedings of the National Academy of Sciences* 111(22):8025–30. Retrieved March 2, 2017 (http://www.ncbi.nlm.nih.gov/pubmed/24843152).

Ma, Wanlong et al. 2010. "JAK2 Exon 14 Deletion in Patients with Chronic Myeloproliferative Neoplasms" edited by A. Navarro. *PLoS ONE* 5(8):e12165. Retrieved April 22, 2017 (http://dx.plos.org/10.1371/journal.pone.0012165).

Ma, Xianyue and Peter P. Sayeski. 2004. "Vaccinia Virus-Mediated High Level Expression and Single Step Purification of Recombinant Jak2 Protein." *Protein Expression and Purification* 35(2):181–89. Retrieved January 13, 2017 (http://www.ncbi.nlm.nih.gov/pubmed/15135391).

Maurel, Damien et al. 2008. "Cell-Surface Protein-Protein Interaction Analysis with

Time-Resolved FRET and Snap-Tag Technologies: Application to GPCR Oligomerization." *Nature Methods* 5(6):561–67. Retrieved April 2, 2017 (http://www.ncbi.nlm.nih.gov/pubmed/18488035).

Miller, Lawrence W., Yunfei Cai, Michael P. Sheetz, and Virginia W. Cornish. 2005. "In Vivo Protein Labeling with Trimethoprim Conjugates: A Flexible Chemical Tag." *Nature Methods* 2(4):255–57. Retrieved April 23, 2017 (http://www.nature.com/doifinder/10.1038/nmeth749).

Min, Xiaoshan et al. 2015. "Structural and Functional Characterization of the JH2 Pseudokinase Domain of JAK Family Tyrosine Kinase 2 (TYK2)." *Journal of Biological Chemistry* 290(45):27261–70. Retrieved March 5, 2017 (http://www.ncbi.nlm.nih.gov/pubmed/26359499).

Nathalie George, †, † Horst Pick, † Horst Vogel, ‡ and Nils Johnsson, and † Kai Johnsson*. 2004. "Specific Labeling of Cell Surface Proteins with Chemically Diverse Compounds." Retrieved April 23, 2017 (http://pubs.acs.org/doi/abs/10.1021/ja048396s).

O'Hare, T. et al. 2005. "In Vitro Activity of Bcr-Abl Inhibitors AMN107 and BMS-354825 against Clinically Relevant Imatinib-Resistant Abl Kinase Domain Mutants." *Cancer Research* 65(11):4500–4505. Retrieved April 22, 2017 (http://www.ncbi.nlm.nih.gov/pubmed/15930265).

O'Shea, J. J., M. Gadina, and Y. Kanno. 2011. "Cytokine Signaling: Birth of a Pathway." *The Journal of Immunology* 187(11):5475–78. Retrieved December 19, 2016 (http://www.ncbi.nlm.nih.gov/pubmed/22102730).

O'Shea, John J., Apostolos Kontzias, Kunihiro Yamaoka, Yoshiya Tanaka, and Arian Laurence. 2013. "Janus Kinase Inhibitors in Autoimmune Diseases." *Annals of the Rheumatic Diseases* 72 Suppl 2(0 2):ii111-5. Retrieved March 24, 2017 (http://www.ncbi.nlm.nih.gov/pubmed/23532440).

Passamonti, F. et al. 2008. "Prognostic Factors for Thrombosis, Myelofibrosis, and Leukemia in Essential Thrombocythemia: A Study of 605 Patients." *Haematologica* 93(11):1645–51. Retrieved April 22, 2017 (http://www.ncbi.nlm.nih.gov/pubmed/18790799).

Passamonti, Francesco and Elisa Rumi. 2009. "Clinical Relevance of JAK2 (V617F) Mutant Allele Burden." *Haematologica* 94(1):7–10. Retrieved April 22, 2017 (http://www.ncbi.nlm.nih.gov/pubmed/19118374).

Periasamy, Ammasi., Richard N. Day, and American Physiological Society. 2005. *Molecular Imaging : FRET Microscopy and Spectroscopy*. Published for the American Physiological Society by Oxford University Press. Retrieved April 2, 2017 (https://books.google.fi/books?id=K0aawJ6sX-sC&pg=PA72&redir_esc=y#v=onepage&q&f=false).

Pesu, Marko et al. 2008. "Therapeutic Targeting of Janus Kinases." *Immunological Reviews* 223(1):132–42. Retrieved March 24, 2017 (http://www.ncbi.nlm.nih.gov/pubmed/18613833).

Phizicky, E. M. and S. Fields. 1995. “Protein-Protein Interactions: Methods for Detection and Analysis.” *Microbiological Reviews* 59(1):94–123. Retrieved April 2, 2017 (http://www.ncbi.nlm.nih.gov/pubmed/7708014).

Pietra, Daniela et al. 2008. “Somatic Mutations of JAK2 Exon 12 in Patients with JAK2 (V617F)-Negative Myeloproliferative Disorders.” *Blood* 111(3). Retrieved April 22, 2017 (http://www.bloodjournal.org/content/111/3/1686?sso-checked=true).

Rane, Sushil G. and E.Premkumar Reddy. 2000. “Janus Kinases: Components of Multiple Signaling Pathways.” *Oncogene* 19(49):5662–79. Retrieved December 20, 2016 (http://www.nature.com/doifinder/10.1038/sj.onc.1203925).

Rawlings, Jason S., Kristin M. Rosler, and Douglas A. Harrison. 2004. “The JAK/STAT Signaling Pathway.” *Journal of Cell Science* 117(8).

Roy, Rahul, Sungchul Hohng, and Taekjip Ha. 2008. “A Practical Guide to Single-Molecule FRET.” *Nature Methods* 5(6):507–16. Retrieved April 25, 2017 (http://www.nature.com/doifinder/10.1038/nmeth.1208).

Russell, S. M. et al. 1995. “Mutation of Jak3 in a Patient with SCID: Essential Role of Jak3 in Lymphoid Development.” *Science (New York, N.Y.)* 270(5237):797–800. Retrieved January 27, 2017 (http://www.ncbi.nlm.nih.gov/pubmed/7481768).

Saharinen, P. and O. Silvennoinen. 2002. “The Pseudokinase Domain Is Required for Suppression of Basal Activity of Jak2 and Jak3 Tyrosine Kinases and for Cytokine-Inducible Activation of Signal Transduction.” *Journal of Biological Chemistry* 277(49):47954–63. Retrieved January 16, 2017 (http://www.ncbi.nlm.nih.gov/pubmed/12351625).

Saharinen, P., K. Takaluoma, and O. Silvennoinen. 2000. “Regulation of the Jak2 Tyrosine Kinase by Its Pseudokinase Domain.” *Molecular and Cellular Biology* 20(10):3387–95. Retrieved January 16, 2017 (http://www.ncbi.nlm.nih.gov/pubmed/10779328).

Scott, L. M., Mike A. Scott, Peter J. Campbell, and Anthony R. Green. 2006. “Progenitors Homozygous for the V617F Mutation Occur in Most Patients with Polycythemia Vera, but Not Essential Thrombocythemia.” *Blood* 108(7):2435–37. Retrieved April 22, 2017 (http://www.ncbi.nlm.nih.gov/pubmed/16772604).

Sekar, Rajesh Babu and Ammasi Periasamy. 2003. “Fluorescence Resonance Energy Transfer (FRET) Microscopy Imaging of Live Cell Protein Localizations.” *The Journal of Cell Biology* 160(5):629–33. Retrieved April 25, 2017 (http://www.ncbi.nlm.nih.gov/pubmed/12615908).

Shan, Yibing et al. 2014. “Molecular Basis for Pseudokinase-Dependent Autoinhibition of JAK2 Tyrosine Kinase.” *Nature Structural & Molecular Biology* 21(7):579–84. Retrieved January 13, 2017 (http://www.ncbi.nlm.nih.gov/pubmed/24918548).

Shcherbakova, Daria M., Mark A. Hink, Linda Joosen, Theodorus W. J. Gadella, and Vladislav V. Verkhusha. 2012. “An Orange Fluorescent Protein with a Large Stokes Shift for Single-Excitation Multicolor FCCS and FRET Imaging.” *Journal of the American Chemical Society* 134(18):7913–23. Retrieved April 23, 2017

(http://www.ncbi.nlm.nih.gov/pubmed/22486524).

Shimomura, O. 1979. “Structure of the Chromophore of *Aequorea* Green Fluorescent Protein.” *FEBS Letters* 104(2):220–22. Retrieved April 23, 2017 (http://doi.wiley.com/10.1016/0014-5793%2879%2980818-2).

Silvennoinen, O. and S. R. Hubbard. 2015. “Molecular Insights into Regulation of JAK2 in Myeloproliferative Neoplasms.” *Blood* 125(22):3388–92. Retrieved December 22, 2016 (http://www.ncbi.nlm.nih.gov/pubmed/25824690).

Silvennoinen, Olli et al. 2013. “New Insights into the Structure and Function of the Pseudokinase Domain in JAK2.” *Biochemical Society Transactions* 41(4):1002–7. Retrieved January 27, 2017 (http://www.ncbi.nlm.nih.gov/pubmed/23863170).

Silver, Richard T. et al. 2011. “JAK2V617F Allele Burden in Polycythemia Vera Correlates with Grade of Myelofibrosis, but Is Not Substantially Affected by Therapy.” *Leukemia Research* 35(2):177–82. Retrieved April 22, 2017 (http://www.ncbi.nlm.nih.gov/pubmed/20650526).

Sino Biological Inc. n.d. “Cytokine Signalling.” Retrieved December 19, 2016 (http://www.sinobiological.com/Cytokine-Signaling-Cytokine-Signalling-a-5799.html).

Soh, Nobuaki. 2008. “Selective Chemical Labeling of Proteins with Small Fluorescent Molecules Based on Metal-Chelation Methodology.” 1004–24.

Spagnuolo, Carla C., Rudolf J. Vermeij, and Elizabeth A. Jares-Erijman. 2006. “Improved Photostable FRET-Competent Biarsenical−Tetracysteine Probes Based on Fluorinated Fluoresceins.” Retrieved April 25, 2017 (http://pubs.acs.org/doi/abs/10.1021/ja063212q).

Sun, Yue-Ming and Yue-Ming Sun. 2014. “The IL-6/JAK/STAT3 Pathway: Potential Therapeutic Strategies in Treating Colorectal Cancer (Review).” *International Journal of Oncology* 44(4):1032–40. Retrieved December 22, 2016 (http://www.ncbi.nlm.nih.gov/pubmed/24430672).

Tanner, J. W., W. Chen, R. L. Young, G. D. Longmore, and A. S. Shaw. 1995. “The Conserved Box 1 Motif of Cytokine Receptors Is Required for Association with JAK Kinases.” *The Journal of Biological Chemistry* 270(12):6523–30. Retrieved January 19, 2017 (http://www.ncbi.nlm.nih.gov/pubmed/7896787).

Tayal, Vandana and Bhupinder Singh Kalra. 2008. “Cytokines and Anti-Cytokines as Therapeutics — An Update.” *European Journal of Pharmacology* 579(1):1–12.

Tokarski, John S. et al. 2006. “The Structure of Dasatinib (BMS-354825) Bound to Activated ABL Kinase Domain Elucidates Its Inhibitory Activity against Imatinib-Resistant ABL Mutants.” *Cancer Research* 66(11). Retrieved April 22, 2017 (http://cancerres.aacrjournals.org/content/66/11/5790.long).

Toms, Angela V et al. 2013. “Structure of a Pseudokinase-Domain Switch That Controls Oncogenic Activation of Jak Kinases.” *Nature Structural & Molecular Biology* 20(10):1221–23. Retrieved March 9, 2017

(http://www.nature.com/doifinder/10.1038/nsmb.2673).

Tour, Oded et al. 2007. “Calcium Green FlAsH as a Genetically Targeted Small-Molecule Calcium Indicator.” *Nature Chemical Biology* 3(7):423–31. Retrieved April 25, 2017 (http://www.nature.com/doifinder/10.1038/nchembio.2007.4).

Vaiyapuri, Periasamy S., Alshatwi A. Ali, Akbarsha A. Mohammad, Jeyalakshmi Kandhavelu, and Meenakshisundaram Kandhavelu. 2015. “Time Lapse Microscopy Observation of Cellular Structural Changes and Image Analysis of Drug Treated Cancer Cells to Characterize the Cellular Heterogeneity.” *Environmental Toxicology* 30(6):724–34. Retrieved January 13, 2016 (http://www.ncbi.nlm.nih.gov/pubmed/24446218).

VanderKuur, J. A. et al. 1994. “Domains of the Growth Hormone Receptor Required for Association and Activation of JAK2 Tyrosine Kinase.” *The Journal of Biological Chemistry* 269(34):21709–17. Retrieved January 18, 2017 (http://www.ncbi.nlm.nih.gov/pubmed/8063815).

Verstovsek, Srdan et al. 2012. “A Double-Blind, Placebo-Controlled Trial of Ruxolitinib for Myelofibrosis.” *New England Journal of Medicine* 366(9):799–807. Retrieved April 22, 2017 (http://www.nejm.org/doi/abs/10.1056/NEJMoa1110557).

Visser, Antonie J. W. G., Eugene S. Vysotski, and John Lee. 2011. “Critical Transfer Distance Determination Between FRET Pairs.” Retrieved April 2, 2017 (http://photobiology.info/Experiments/Biolum-Expt.html).

Wang, Xinquan, Patrick Lupardus, Sherry L. LaPorte, and K.Christopher Garcia. 2009. “Structural Biology of Shared Cytokine Receptors.” *Annual Review of Immunology* 27:29.

Wombacher, Richard and Virginia W. Cornish. 2011. “Chemical Tags: Applications in Live Cell Fluorescence Imaging.” *Journal of Biophotonics* 4(6):391–402. Retrieved April 23, 2017 (http://doi.wiley.com/10.1002/jbio.201100018).

Yamaoka, Kunihiro et al. 2004. “The Janus Kinases (Jaks).” *Genome Biology* 5(12):253. Retrieved December 20, 2016 (http://www.ncbi.nlm.nih.gov/pubmed/15575979).

Yang, Fan, Larry G. Moss, and George N. Phillips. 1996. “The Molecular Structure of Green Fluorescent Protein.” *Nature Biotechnology* 14(10):1246–51. Retrieved April 23, 2017 (http://www.ncbi.nlm.nih.gov/pubmed/9631087).

Zal, Tomasz and Nicholas R. J. Gascoigne. 2004. “Photobleaching-Corrected FRET Efficiency Imaging of Live Cells.” *Biophysical Journal* 86(6):3923–39. Retrieved May 21, 2017 (http://www.ncbi.nlm.nih.gov/pubmed/15189889).

Zand, Martin S. et al. 2013. “Tofacitinab in Renal Transplantation.” *Transplantation Reviews* 27(3):85–89. Retrieved March 25, 2017 (http://linkinghub.elsevier.com/retrieve/pii/S0955470X13000529).

Zhang, Jun-Ming and Jianxiong An. 2007. “Cytokines, Inflammation, and Pain.”

*International Anesthesiology Clinics* 45(2):27–37. Retrieved December 19, 2016 (http://www.ncbi.nlm.nih.gov/pubmed/17426506).

# APPENDIX A

***Table 1.*** *JH2-JH1 DNA and amino acid sequences.*

```
      atggtgtttcacaaaatcagaaatgaagatttgatatttaatgaaagccttggccaaggc
535    M  V  F  H  K  I  R  N  E  D  L  I  F  N  E  S  L  G  Q  G   554
      acttttacaaagatttttaaaggcgtacgaagagaagtaggagactacggtcaactgcat
555    T  F  T  K  I  F  K  G  V  R  R  E  V  G  D  Y  G  Q  L  H   574
      gaaacagaagttctttttaaaagttctggataaagcacacagaaactattcagagtctttc
575    E  T  E  V  L  L  K  V  L  D  K  A  H  R  N  Y  S  E  S  F   594
      tttgaagcagcaagtatgatgagcaagctttctcacaagcatttggttttaaattatgga
595    F  E  A  A  S  M  M  S  K  L  S  H  K  H  L  V  L  N  Y  G   614
      gtatgtgtctgtggagacgagaatattctggttcaggagtttgtaaaatttggatcacta
615    V  C  V  C  G  D  E  N  I  L  V  Q  E  F  V  K  F  G  S  L   634
      gatacatatctgaaaaagaataaaaattgtataaatatattatggaaacttgaagttgct
635    D  T  Y  L  K  K  N  K  N  C  I  N  I  L  W  K  L  E  V  A   654
      aaacagttggcatgggccatgcattttctagaagaaaacacccttattcatgggaatgta
655    K  Q  L  A  W  A  M  H  F  L  E  E  N  T  L  I  H  G  N  V   674
      tgtgccaaaaatattctgcttatcagagaagaagacaggaagacaggaaatcctcctttc
675    C  A  K  N  I  L  L  I  R  E  E  D  R  K  T  G  N  P  P  F   694
      atcaaacttagtgatcctggcattagtattacagttttgccaaaggacattcttcaggag
695    I  K  L  S  D  P  G  I  S  I  T  V  L  P  K  D  I  L  Q  E   714
      agaataccatgggtaccacctgaatgcattgaaaatcctaaaaatttaaatttggcaaca
715    R  I  P  W  V  P  P  E  C  I  E  N  P  K  N  L  N  L  A  T   734
      gacaaatggagttttggtaccactttgtgggaaatctgcagtggaggagataaacctcta
735    D  K  W  S  F  G  T  T  L  W  E  I  C  S  G  G  D  K  P  L   754
      agtgctctggattctcaaagaaagctacaattttatgaagataggcatcagcttcctgca
755    S  A  L  D  S  Q  R  K  L  Q  F  Y  E  D  R  H  Q  L  P  A   774
      ccaaagtgggcagaattagcaaaccttataaataattgtatggattatgaaccagatttc
775    P  K  W  A  E  L  A  N  L  I  N  N  C  M  D  Y  E  P  D  F   794
      aggccttctttcagagccatcatacgagatcttaacagtttgtttactccagattatgaa
795    R  P  S  F  R  A  I  I  R  D  L  N  S  L  F  T  P  D  Y  E   814
      ctattaacagaaaatgacatgttaccaaatatgaggataggtgccctggggttttctggt
815    L  L  T  E  N  D  M  L  P  N  M  R  I  G  A  L  G  F  S  G   834
      gcctttgaagaccgggatcctacacagtttgaagagagacatttgaaatttctacagcaa
835    A  F  E  D  R  D  P  T  Q  F  E  E  R  H  L  K  F  L  Q  Q   854
      cttggcaagggtaatttttgggagtgtggagatgtgccggtatgaccctctacaggacaac
855    L  G  K  G  N  F  G  S  V  E  M  C  R  Y  D  P  L  Q  D  N   874
      actggggaggtggtcgctgtaaaaaagcttcagcatagtactgaagagcacctaagagac
875    T  G  E  V  V  A  V  K  K  L  Q  H  S  T  E  E  H  L  R  D   894
      tttgaaagggaaattgaaatcctgaaatccctacagcatgacaacattgtaaagtacaag
895    F  E  R  E  I  E  I  L  K  S  L  Q  H  D  N  I  V  K  Y  K   914
      ggagtgtgctacagtgctggtcggcgtaatctaaaattaattatggaatatttaccatat
915    G  V  C  Y  S  A  G  R  R  N  L  K  L  I  M  E  Y  L  P  Y   934
      ggaagtttacgagactatcttcaaaaacataaagaacggatagatcacataaaacttctg
935    G  S  L  R  D  Y  L  Q  K  H  K  E  R  I  D  H  I  K  L  L   954
      cagtacacatctcagatatgcaagggtatggagtatcttggtacaaaaaggtatatccac
955    Q  Y  T  S  Q  I  C  K  G  M  E  Y  L  G  T  K  R  Y  I  H   974
      agggatctggcaacgagaaatatattggtggagaacgagaacagagttaaaattggagat
975    R  D  L  A  T  R  N  I  L  V  E  N  E  N  R  V  K  I  G  D   994
      tttgggttaaccaaagtcttgccacaagacaaagaatactataaagtaaaagaacctggt
995    F  G  L  T  K  V  L  P  Q  D  K  E  Y  Y  K  V  K  E  P  G   1014
      gaaagtcccatattctggtatgctccagaatcactgacagagagcaagttttctgtggcc
1015   E  S  P  I  F  W  Y  A  P  E  S  L  T  E  S  K  F  S  V  A   1034
      tcagatgtttggagctttggagtggttctgtatgaacttttcacatacattgagaagagt
1035   S  D  V  W  S  F  G  V  V  L  Y  E  L  F  T  Y  I  E  K  S   1054
      aaaagtccaccagcggaatttatgcgtatgattggcaatgacaaacaaggacagatgatc
1055   K  S  P  P  A  E  F  M  R  M  I  G  N  D  K  Q  G  Q  M  I   1074
      gtgttccatttgatagaacttttgaagaataatggaagattaccaagaccagatggatgc
1075   V  F  H  L  I  E  L  L  K  N  N  G  R  L  P  R  P  D  G  C   1094
      ccagatgagatctatatgatcatgacagaatgctggaacaataatgtaaatcaacgcccc
1095   P  D  E  I  Y  M  I  M  T  E  C  W  N  N  N  V  N  Q  R  P   1114
```

```
      tcctttagggatctagctcttcgagtggatcaaataagggataacatggctggatga
1115  S  F  R  D  L  A  L  R  V  D  Q  I  R  D  N  M  A  G  -     1133
```